

Manufacturing, characteristics and applications of auxetic foams: a state-of-the-art review

JIANG, Wei, REN, Xin, WANG, Shi Long, ZHANG, Xue Gang, ZHANG, Xiang Yu, LUO, Chen, XIE, Yi Min, SCARPA, Fabrizio, ALDERSON, Andrew <<http://orcid.org/0000-0002-6281-2624>> and EVANS, Ken E.

Available from Sheffield Hallam University Research Archive (SHURA) at:

<https://shura.shu.ac.uk/29783/>

This document is the Accepted Version [AM]

Citation:

JIANG, Wei, REN, Xin, WANG, Shi Long, ZHANG, Xue Gang, ZHANG, Xiang Yu, LUO, Chen, XIE, Yi Min, SCARPA, Fabrizio, ALDERSON, Andrew and EVANS, Ken E. (2022). Manufacturing, characteristics and applications of auxetic foams: a state-of-the-art review. *Composites Part B: Engineering*, 235. [Article]

Copyright and re-use policy

See <http://shura.shu.ac.uk/information.html>

1 Manufacturing, characteristics and applications of auxetic foams:

2 A state-of-the-art review

3 **Wei Jiang^a, Xin Ren^{a,*}, Shi Long Wang^a, Xue Gang Zhang^a, Xiang Yu Zhang^a,**
4 **Chen Luo^a, Yi Min Xie^b, Fabrizio Scarpa^c, Andrew Alderson^d, Ken E. Evans^e**

5 ^a College of Civil Engineering, Nanjing Tech University, Nanjing, Jiangsu, 211816, PR China

6 ^b Centre for Innovative Structures and Materials, School of Engineering, RMIT University, Melbourne, 3001,
7 Australia

8 ^c Bristol Composites Institute, University of Bristol, BS8 1TR Bristol, United Kingdom

9 ^d Materials and Engineering Research Institute, Sheffield Hallam University, Sheffield, United Kingdom

10 ^e College of Engineering, Mathematics and Physical Sciences, University of Exeter, EX4 4QF Exeter, United
11 Kingdom

12
13 * Corresponding author: Xin Ren. Email: xin.ren@njtech.edu.cn

14 **Abstract:**

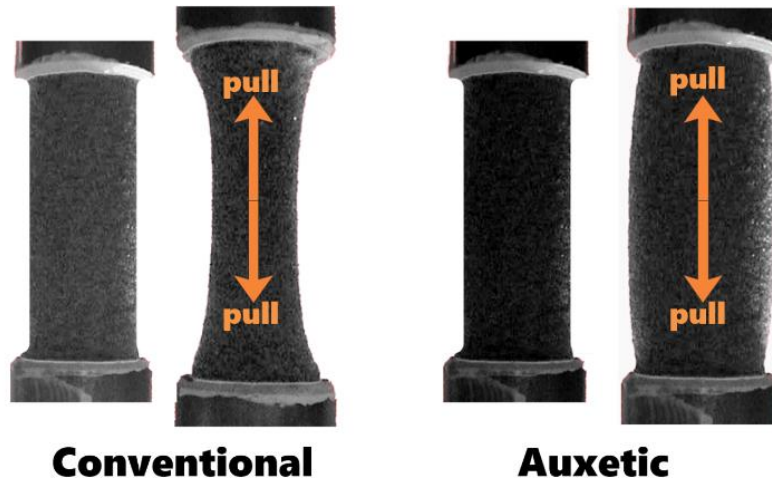
15 Auxetic foams counter-intuitively expand (shrink) under stretching (compression). These
16 foams can exhibit superior mechanical properties such as resistance to shear and indentation,
17 improved toughness and energy absorption (EA) under several types of loadings. Their unique
18 deformation mechanism and manufacturing process lead to special multiphysics properties such as
19 variable permeability, synclastic curvature and shape memory. Except for traditional energy
20 absorber stuff, the potential applications of auxetic foams have involved biomedicine, aerospace,
21 smart sensing, etc. However, most of the potential applications are restrained in the theoretical stage
22 due to complicated fabrication and a deficiency of stability. For removing the barrier for practical
23 application, a series of issues remain to be resolved, though the explorations of the improved
24 conversion methodologies and potential applications are fruitful in the past decades. We present
25 here a review article discussing the state-of-the-art for manufacturing, characterization and
26 applications of auxetic foams. We also provide a view of the existing challenges and possible future
27 research directions, aiming to state the perspective and inspire researchers to further develop the
28 field of auxetic foams.

29 **Keywords: auxetic, foam materials, smart materials, negative Poisson's ratio, protection**
30 **equipment**

31 32 **1. Introduction**

33 The Poisson's ratio (denoted ν for isotropic materials) is a parameter that defines the ratio
34 between the lateral deformation of a body subjected to axial loading, i.e., between the transverse
35 strain (ε_t) and the longitudinal strain (ε_l) with the minus sign ($-\varepsilon_t/\varepsilon_l$ [1]). According to the classical
36 theory of elasticity, the Poisson's ratio for isotropic materials ranges from -1 to 0.5 [2], so that a
37 negative Poisson's ratio is allowable in linear elastic and thermodynamically correct materials. Most
38 of normal materials become fat (thin) under compression (tension), and so exhibit a positive
39 Poisson's ratio behaviour. In contrast, negative Poisson's ratio materials show a counter-intuitive

40 behaviour under axial loading - they become thin (fat) under compression (tension) (**Figure. 1**).

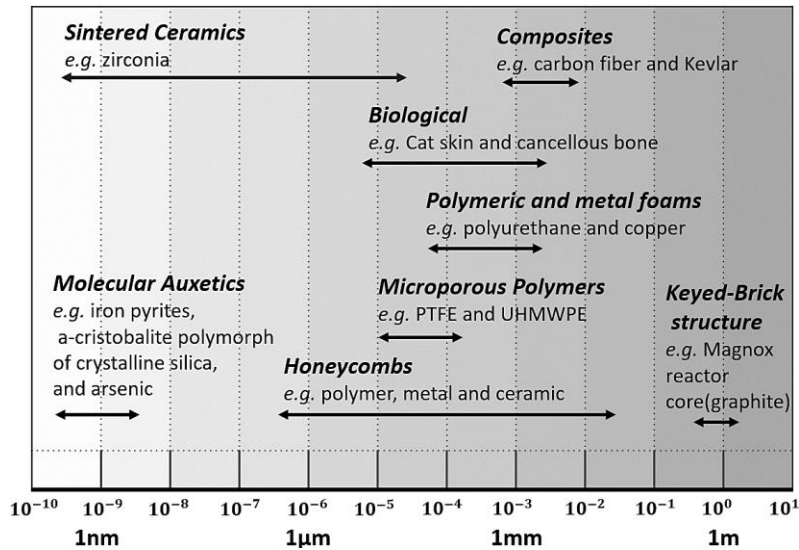


41 **Figure. 1.** Shape changes under stretching of conventional foams (left) and auxetic foams (right).
42

43 The term “auxetic” was introduced by Evans [3] who adapted the ancient Greek word “auxetos”
44 (that which tends to increase) for negative Poisson’s ratio materials. Iron pyrite monocrystals was
45 reported as possessing an auxetic behavior since 1882 [2], with a Poisson’s ratio value of - 1/7
46 estimated by Love [4]. Natural auxetic materials that have been reported in open literature also
47 include cow teat skin [5], cat skin [6], cancellous bone [7] and membranes found in the cytoskeleton
48 of red blood cells [8]. Wojciechowski [9] also demonstrated the existence of negative Poisson’s
49 ratio in cyclic hexamers molecule assemblies subjected to critical pressure levels.

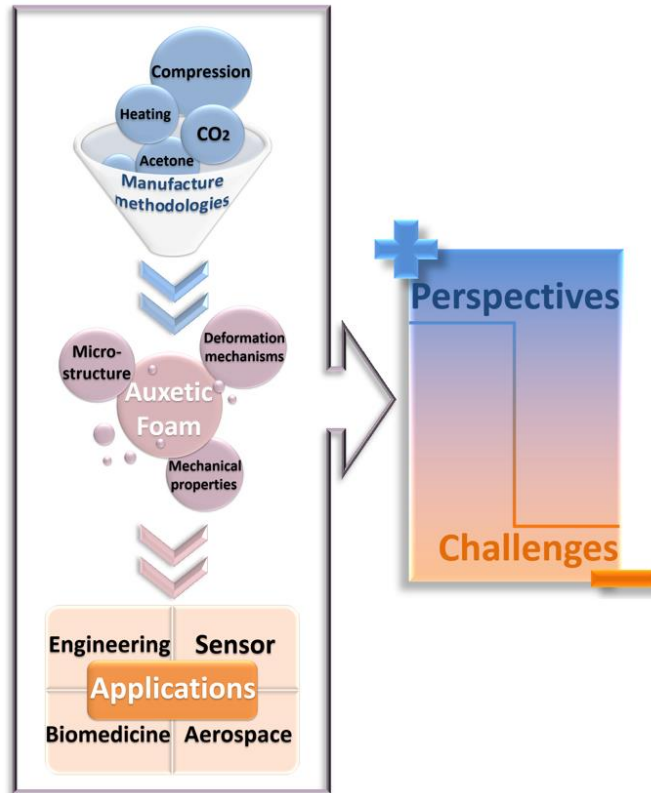
50 Foam materials possess many superior properties, such as improved performance under the
51 impact, lightweight, cost-effective, reusable, desirable acoustic capability, and remarkable chemical
52 and physical stability [10-14]. In this context, foam material has been widely used in daily life and
53 is considered a potential candidate for multifunctional engineering materials. On the other hand,
54 foam materials have high resilience and can bear large strain deformation. Such properties are
55 desirable to auxetic materials which need enough axial deformation for the showing of unique lateral
56 deformation. Therefore, it could be expected that foam material would exhibit more remarkable and
57 functional properties if it be endowed with auxetic performance.

58 The first artificial auxetic open cell foam fabricated using a combination of volumetric
59 compression and thermoforming was reported by Lakes in 1987 [15]. During the following decades,
60 increasing numbers of artificial auxetic materials have been developed at different scales [16]
61 (**Figure. 2**) and one typical methodology, pattern scale factor (PSF) methodology was proposed to
62 artificially design the auxetic unit cells with tunable mechanical performance [17, 18]. A good
63 portion of artificial auxetic materials is fabricated via textiles or 3D printing, whereas auxetic foams
64 can be produced by post-processing existing conventional off-the-shelf porous materials.



65
66 **Figure. 2.** Categories of auxetics at different scales (Reproduced from [19]).

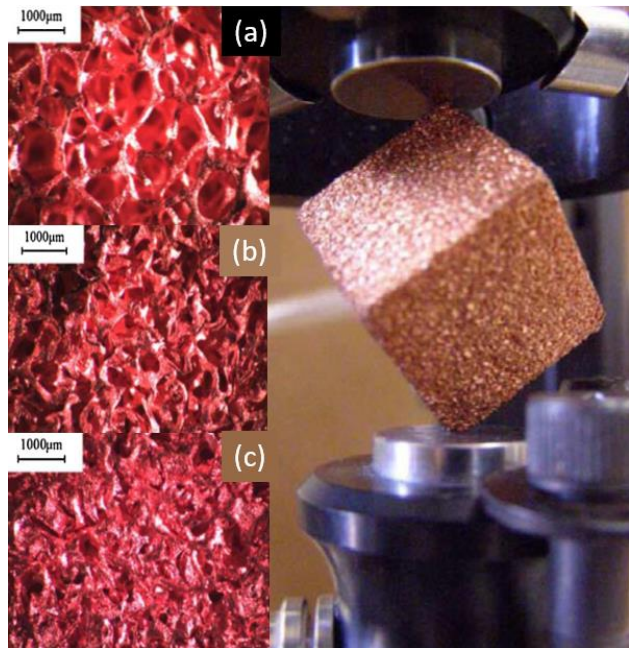
67 Though several reviews on auxetic materials have been published in the past decades [16, 19-
68 28], a more focused review on auxetic foams is still rare. Considerable progress in the fabrication,
69 characterization and applications of auxetic foams has been reported in the past eight years since
70 the publication of last review on auxetic foams [29]. In this paper, state-of-the-art review and the
71 problems accompanied with possible solutions of current researches on the manufacture,
72 characteristics and applications of auxetic foams have been made, aiming to inspire the peers and
73 pave the way for further studies (**Figure. 3**).



74
75 **Figure. 3.** Outline of this article.
76

77 **2. Manufacture methodologies for auxetic foams**

78 The principle for transforming traditional foams into auxetic form consists in producing a
79 stable compression that induces the lattice into a re-entrant shape. The volumetric compression can
80 be generated either by mechanical or via air pressure at first, and the foams ribs can then be softened
81 into shape by applying a specific heating profile or chemical solvent, followed by the re-entrant
82 shape fixed by the annealing and a cooling stage. Softening and cooling are however unnecessary
83 for metal foams (copper foam) (**Figure. 4**) [30-33] due to the high plasticity and the possibility of
84 creating the re-entrant shape by plastic deformations only. Methodologies for the conversion of
85 auxetic foams are fruitful and still on-going, current foam materials that can be converted into
86 auxetics are listed in **Table. 1**.



87 **Figure. 4.** Microstructures of copper foam subjected to volumetric compression ratios (VCR: Initial /
88 Final Volume) of (a) 1, (b) 4.43 and (c) 4.94 respectively (Adapted from [33]).

90 **Table. 1.** Examples of several foam samples that have been managed to be converted into auxetics

(“ppi” means “pores per inch” - the most common unit for foam pore size).

material	pore diameter (mm)	density (kg/m ³)	reference	
polyester urethane foam	closed-cell	0.42 (60 ppi)	37.9 [37]	
	reticulated	0.42 (60 ppi)	33.7 [37]	
	open-cell	2.54 (10 ppi)	24.1	
		0.85 (30 ppi)	24.5	[37]
		0.42 (60 ppi)	21.7	
open-cell polyurethane foam	2.54 (10 ppi)	34	[70]	
	1.27 (20 ppi)	30	[66]	
	0.73-0.85 (30-35 ppi)	32	[113]	
	0.73-0.85 (30-35 ppi)	27	[144]	
	0.56 (45 ppi)	27	[70]	
	0.45-0.49 (52-57 ppi)	27	[38]	
	0.39 (65 ppi)	30	[66]	
	0.25 (100 ppi)	30	[66]	
closed-cell polyethylene foam	20 (expansion ratio)	not given		
	30 (expansion ratio)	not given	[53]	
	45 (expansion ratio)	not given		
closed-cell polyvinyl chloride (PVC) foam	not given	52	[53]	
open-cell copper foam	1	not given	[30]	
room temperature vulcanizing elastomeric silicone foam	not given	150	[30]	
closed-cell polymethacrylimide foam	not given	52		
	not given	205	[44]	
	not given	301		
closed-cell polyethylene foam	not given	59		
	not given	109	[44]	
	not given	158		

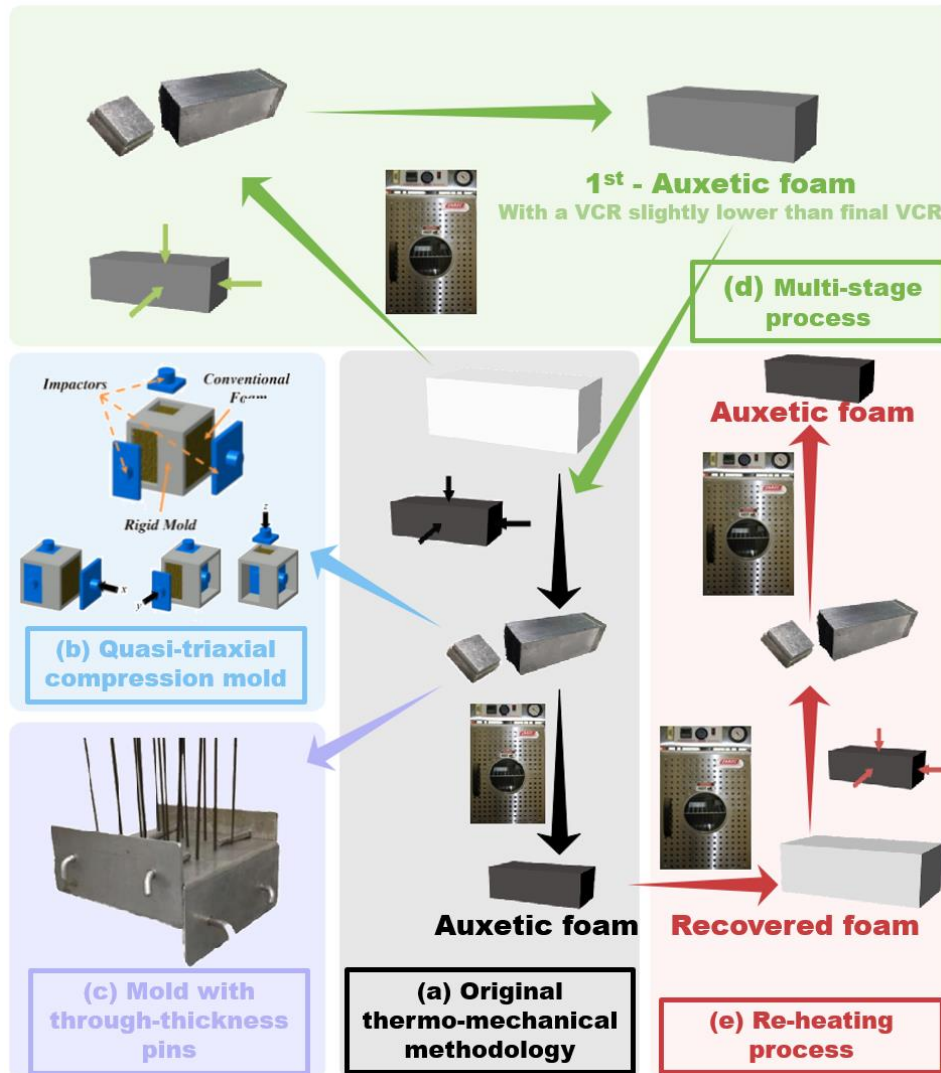
93 2.1 Original and improved thermo-mechanical methodologies

94 In 1987, the first auxetic foam with Poisson’s ratio value of - 0.7 was converted from
 95 conventional commercial open-cell polyurethane (PU) foam by Lakes [15] through a thermo-
 96 mechanical (mechanical compression and thermoforming) methodology (**Figure. 5a**). Samples of
 97 conventional foam were compressed along three orthogonal directions and placed in a mold at a
 98 temperature slightly higher than the softening one of the foam samples (163°C to 171°C). The mold
 99 was then cooled and the resulting foam showed stable buckled ribs and negative Poisson’s ratio.
 100 Uniaxial compression was also applied but could only enable the production of foams with a near
 101 zero Poisson’s ratio rather than a negative value [15]. However, further studies have shown that
 102 foam samples that are sufficiently thin could provide a negative but inhomogeneous distributed
 103 Poisson’s ratio under only uniaxial compression [34, 35].

104 The thermo-mechanical methodology could also convert polyvinyl chloride (PVC) foams [36,
 105 37], closed-cell PU [38] and silicone rubber foam [30] into auxetic foam. As for metal foam (copper
 106 foam), the heating stage is however not necessary because the conversion could happen under
 107 sequential plastic compression along three directions [30-33]. Friis *et al.* [30] produced auxetic PU
 108 foam by applying triaxial compression during the foaming process without the heating phase as well.

109 The toughest manufacturing limitations of the thermo-mechanical methodology are, especially
 110 in manufacturing large foam samples, the sufficiency of long-term stability in mechanical properties,
 111 risk of creasing surface and uneven heating and / or compression during manufacturing. To

112 overcome these drawbacks, several improvements based on the thermo-mechanical methodology
113 have been introduced (**Figure. 5**). A quasi tri-axial methodology (**Figure. 5b**) was described by
114 Mohsenizadeh *et al.* [39]. A novel mold was introduced to split the compression process into three
115 stages (x-compression, y-compression and z-compression), ensuring that foam samples are evenly
116 compressed in three directions. Foam samples fabricated using this methodology showed a better
117 homogeneity, rigidity and isotropic behaviour and effectively overcame the surface creasing
118 problem. Duncan *et al.* [40] developed a novel cuboidal mold with through-thickness pins (**Figure.**
119 **5c**) to reduce folds on the foam surface and improve the uniformity of compression throughout the
120 sample. The use of pins to control the internal compression state of the foam, in addition to the
121 external compression applied by the mold, was first introduced by Sanami *et al.* in the production
122 of one-piece radially gradient “core-sheath” foams having distinctly different core and sheath region
123 pore structures, Poisson’s ratios (including negative), and Young’s moduli [41]. Subsequently,
124 Duncan *et al.* [42] designed a novel mold with partly distributed through-thickness pins for
125 fabricating gradient auxetic foam sheets. This mold was partitioned to generate different fabrication
126 and compression processes, which could significantly shorten the manufacturing time of different
127 types of foam samples. The work of Duncan *et al.* also highlighted the advantages brought by
128 through-thickness pins approach. Except for introducing novel molds to improve compression
129 quality, some additional processes are also effective to obtain auxetic foam samples with better
130 performance in stability and mechanical properties. Chan *et al.* [38] proposed a multi-stage process
131 enabling conventional foam samples to be converted twice in different VCR (**Figure. 5d**) for a
132 gradual compression. This process can effectively avoid the creasing of the surfaces that occurs
133 during original one-stage compression and exhibits the potential benefit to manufacture large foam
134 samples. Bianchi [43, 44] applied a re-heating process (**Figure. 5e**) on the samples recovered from
135 auxetic foams. The stability of the auxeticity and the mechanical properties of the auxetic foam
136 samples could be significantly enhanced by re-manufacturing.

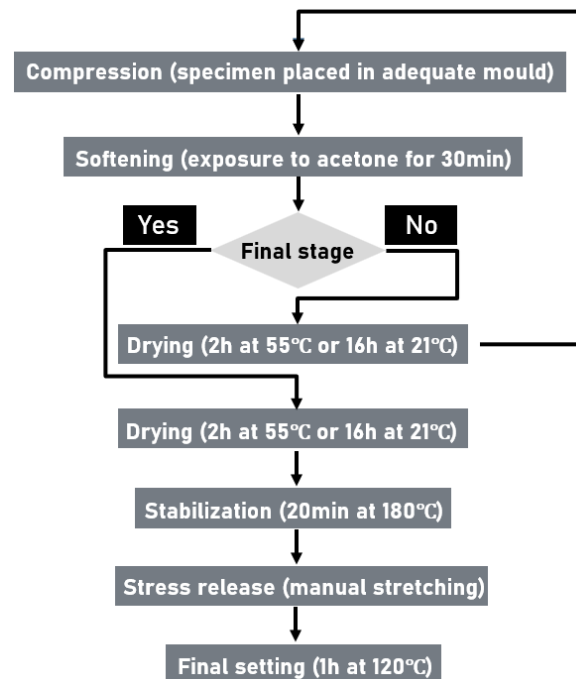


137
 138 **Figure 5.** Current methodologies based on the thermo-mechanical methodology of (a) original thermo-
 139 thermo-mechanical methodology [15], introducing of (b) quasi tri-axial mold [39] and (c) cuboidal mold with
 140 through-thickness pins [40] for uniform compression, (d) adopting a pre-auxetic process to realize
 141 multi-stage (gradual) compression [38], and (e) a double thermo-mechanical process to convert the
 142 recovered foam to obtain twice-processed auxetic foam samples with long-term shape stability [43, 44].

143 Two alternative compression techniques to produce the volumetric compression have been also
 144 elsewhere developed. The early study of Martz *et al.* [45] reported that closed-cell
 145 polymethacrylimide (PMI) and low-density polyethylene (LDPE) foams could show an auxetic
 146 behaviour under high external air pressure followed by heating process. Air pressure (or suction)
 147 was also used in the “half mould” manufacturing process proposed by Bianchi *et al.* [46] to
 148 manufacture auxetic foams samples with curved and arbitrary shapes. By using engineered vacuum,
 149 Zhang *et al.* [47] fabricated foam samples having a stiffness 5 times larger than the stiffest auxetic
 150 foam presented in open literature, meeting the requirements of both high stiffness and auxeticity.
 151 Hydro-static pressure has been also applied by Najarian *et al.* [48] as another tool to compress the
 152 foam samples.

153 **2.2 Adopting of acetone, CO₂, steam penetration and condensation (SPC) and 3D**
154 **printer**

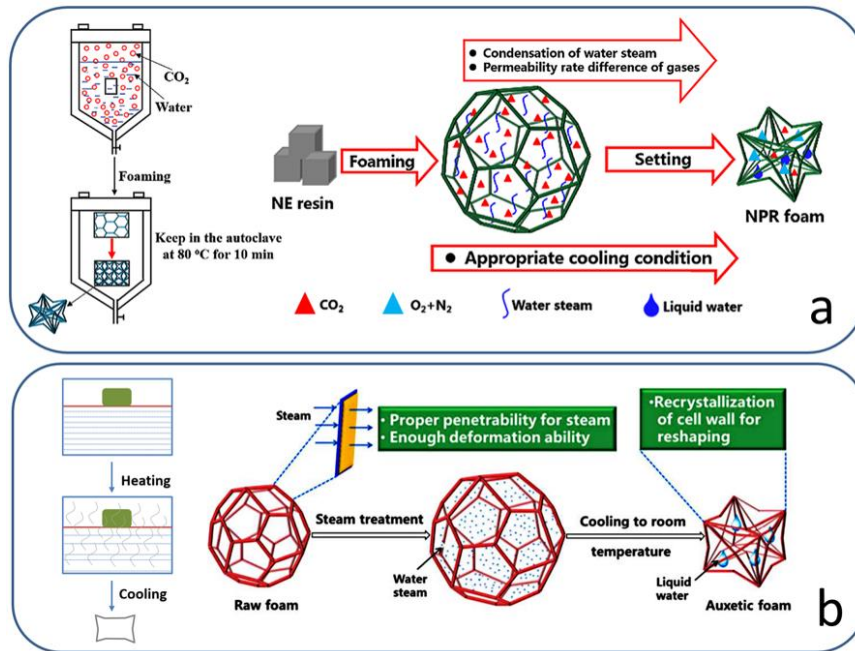
155 One of the earliest explanations of the auxetic behavior in negative Poisson's ratio foams is
156 based on the "missing rib" concept, i.e., the failure and breaking of ribs during the volumetric
157 compression leading to changes of the original pore cell geometry. Smith *et al.* [49] therefore
158 predicted that foam ribs might be removed following a chemical process so the foam samples could
159 turn into auxetics. In 2009, Grima [50] realized the predicted conversion of auxetic foams by placing
160 compressed foam samples within a container in acetone to soften foam ribs, rather than applying a
161 temperature profile for the annealing. Inspired by this novel softening process, an improved chemo-
162 mechanical methodology (the Mechanic-Chemic-Thermal technique) (**Figure. 6**) was then
163 developed by the Air Force Institute of Technology (AFIT) in Poland [51]. Compared with foams
164 fabricated using the original thermo-mechanical methodology [52], auxetic foams softened by
165 chemical process could obtain a lower Poisson's ratio without the risk of uneven heating, and this
166 approach is potential to produce large samples, however in considering of the safety hazard and
167 environmental footprint issues, such chemical softening process is not recommended in further
168 researches.



169 **Figure. 6.** Flow chart depicting the four stages auxetic foam manufacturing process proposed by AFIT
170
171 (Adapted from [51]).

172 For developing a more environment-friendly fabrication process, Li [53] adopted CO₂ as the
173 main softening agent. Carbon dioxide could reduce the glass transition temperature of Styrene
174 acrylonitrile copolymer (SAN) particles (copolymers in PU foams, play the key role in foam ribs
175 softening) after a series of chemical reactions. Auxetic foams treated with carbon dioxide could be
176 rapidly converted at a room temperature and exhibited a nearly constant value of negative Poisson's
177 ratio over a large strain range. Recently, basing on the function of CO₂ in the manufacturing, high-

178 performance closed-cell auxetic nylon elastomer (NE) foams with Poisson's ratio value of - 1.29
 179 and superior mechanical properties have been fabricated by Fan *et al.* [54] using a green and
 180 environment-friendly methodology named One-Pot CO₂ foaming process (**Figure. 7a**). Fan *et al.*
 181 have also remarked that this methodology could be also applied to other polymers (like ethylene-
 182 vinyl acetate (EVA) resins). SPC methodology (**Figure. 7b**) was described by Fan *et al.* [36], which
 183 enabled the development of auxetic closed-cell polyethylene (PE) and PVC foams. This
 184 methodology could also be used for fabricating large auxetic foam samples as a related paper of
 185 Duncan *et al.* [55] shows.



186
 187 **Figure. 7.** Schematic drawings showing the experimental flow chart (left) and possible formation
 188 mechanism (right) of a) One-Pot CO₂ foaming process and b) SPC process (Adapted from [54] and
 189 [36]).

190 With the rapid development of 3D print technology, complicated 3D structures can be
 191 fabricated with increasingly high precision in 3D printers. Except for traditional methodologies to
 192 convert foam materials into auxetics, a novel concept of manufacturing auxetic foams by 3D print
 193 technology was proposed by Critchley *et al.* [56], the foam samples they manufactured were
 194 customized designed and fabricated without any random cell orientation, providing a new
 195 methodology to generate foam structures with stability and homogeneity (**Figure. 8**). However,
 196 relatively high costs, scale limitation and the presence of defects still impede the broad application
 197 of this technique. From this perspective, the rest of porous auxetic structures fabricated by 3D
 198 printers could be defined as a novel foam material in a broad sense (Syntactic foams [28, 57-65]).
 199 Such structures are potential alternatives as polymer foam materials to some applications such as
 200 sensors or soft robots, providing stable and precise reactions under loadings.

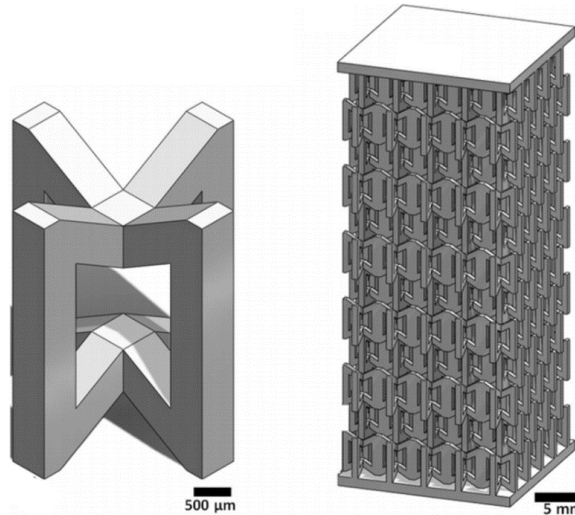


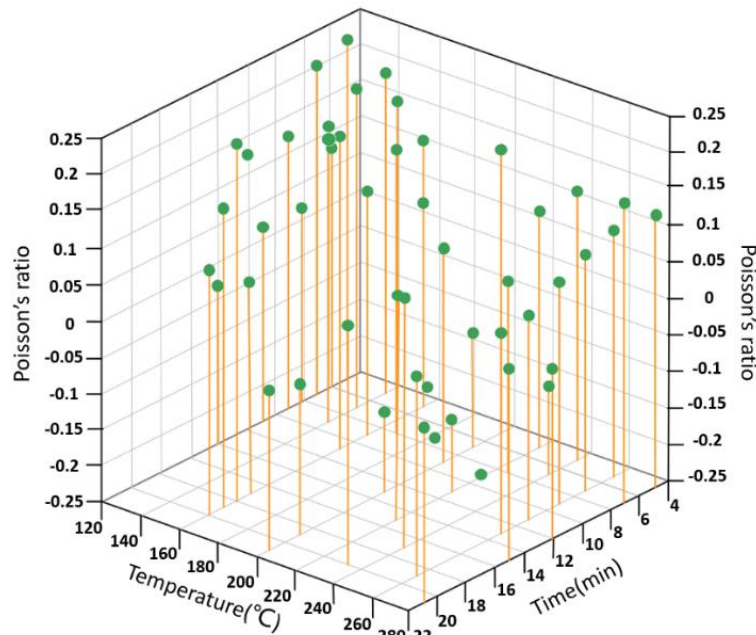
Figure 8. The unit cell (left) and the whole model (right) of auxetic foam fabricated by 3D print technology [56].

Although the methodologies mentioned above are feasible to convert conventional foams into auxetics, most of them are restricted in a small dimension. Large samples cannot be compressed and softened in an even manner, resulting in sometimes substandard performance. Many potential applications for which auxetic foams could be extremely advantageous to use (cushions and pads, for example) are still confined at the stage of design and prototyping, waiting for low-cost and efficient large scale manufacturing routes to be fully developed.

2.3 Parametric manufacturing

Several research teams have looked at identifying the most important manufacturing parameters that improve the quality and performance of auxetic foams. In relation to the thermo-mechanical methodology, the debate about the best combinations of those parameters (temperature, heating time and VCR) has started since the beginning of the original productions of auxetic foams. The first negative Poisson's ratio polymer foam fabricated by Lakes [15] was subjected to VCR values from 1.4 to 4 and heating temperatures between 163°C and 171°C, heating time was however unmentioned in his work. Friis *et al.* [30] indicated that 200°C may be a more suitable temperature to soften the foam ribs for the tested PU foams of solid volume fraction 0.043. The heating time and VCR adopted in the work are 7 min and 3.4, respectively. Wang *et al.* treated 40 100 ppi (pore diameter of 0.25 mm) PU foam specimens (the density was 0.033 g/cm³) under different combinations of manufacturing parameter to investigate the influence of the temperature and heating time on the final value of the Poisson's ratio [66] (**Figure 9**). In the work of Choi *et al.* [67], two types of open-cell PU foams (gray polyurethane-polyester foam: $\rho/\rho_s = 0.03 \pm 10\%$, L (length of cell rib) = 0.4 ± 0.03 mm and Scott industrial foam: $\rho/\rho_s = 0.03 \pm 7\%$, L = 1.2 ± 0.03 mm) have been produced by using different parametrical combinations. The lowest value of the Poisson's ratio achieved in that work was - 0.7, for both kinds of foam, obtained from a VCR between 3.3 to 3.7 under a heating temperature of 170 °C for 17 min. Moreover, another paper of Choi' group shows

228 that the VCR should be smaller than 5 to avoid contact between ribs and adhesion [67].

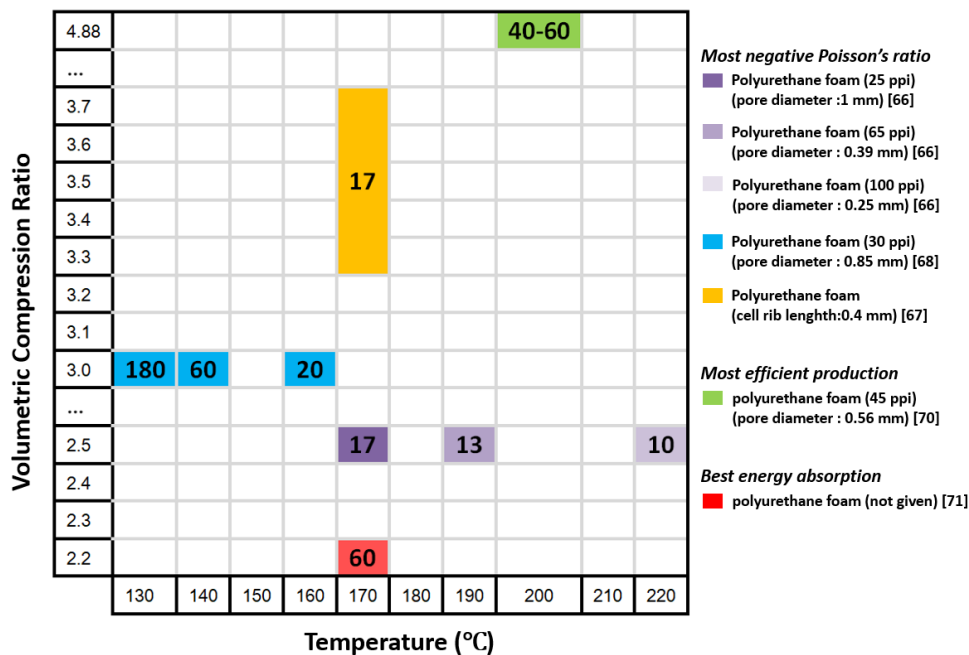


229
230 **Figure. 9.** Poisson's ratio of auxetic foams fabricated from 100 ppi (pore diameter of 0.25 mm) PU
231 foams with VCR of 2.5 and different combinations of temperature and heating time (Data replotted
232 from [66]).

233 Martz *et al.* [45] noted that excessive temperature exposure (220 °C) could only make
234 transformed PMI closed-cell foams stiffer without auxeticity, the reason for this phenomenon may
235 be the adhesion of melted foam walls. Duncan *et al.* [68] reported that a temperature higher than
236 200 °C would however induce a substantial mass loss of the open-cell PUR30FR foams, and a
237 combination of high temperature and long heating times could only make them exhibit auxeticity in
238 tension. The optimal parametrical combination they provided are VCR = 3, 130 °C, 140 °C, and
239 160 °C for 180, 60, and 20 min, respectively, resulting in a minimum $v = -0.2$. As for heating time,
240 Chan and Evans [38] proposed that foam samples could not be “set” and were apt to recover to
241 their original shape (or be melted into a block of dense material) if the heating time was too short
242 (or too long in the case of melting). The critical temperatures of reticulated PU foams in three phases
243 (softening around 180 °C, liquefaction around 270 °C and polymer decomposition around 300 °C)
244 were also noted in the paper. Temperatures about 5 - 20 °C lower than the softening temperature
245 were suggested advisable to maximize the stress relaxation and minimize the possible bonding
246 between cell ribs. Wang and Lakes [66] then proposed a series of optimal combinations of
247 temperature and heating times for open-cell PU foam samples with different cell sizes (25 ppi, 65
248 ppi and 100 ppi, i.e., pore diameter of 1 mm, 0.39 mm and 0.25 mm, respectively). All samples were
249 produced with the same VCR of 2.5. Detailed parameters and results are presented in **Figure. 10**.
250 The first design of experiment (DoE) work related to the manufacturing of open cell PU auxetic
251 foams was carried out by Bianchi *et al.* [69]. The Authors of that work carried a systematic campaign
252 of quasi-static cyclic tension/compression tests on 80 different cylindrical foam specimens with

253 VCRs ranging between 5 and 19, two temperatures (135 °C and 150 °C), two heating times (12 min
 254 and 15 min) and also two different cooling methodologies (water and air ventilation). The final
 255 conclusions of the DoE showed that the VCR is the most statistically important manufacturing,
 256 while no significant statistical correlation could be identified with the temperature, heating times
 257 provided and the cooling methodologies. Critchley *et al.* [70] recently provided an updated
 258 statistical approach for the optimization of the manufacturing parameters to improve the efficiency
 259 of the production. An optimal combination of VCR, porosity and heating time was recommended
 260 for a conversion temperature of 200 °C, detailed parameters are also shown in **Figure. 10**. In view
 261 of practical applications, especially for applications in EA, the final density is however indicated as
 262 a critical parameter [69, 71, 72]. A lower VCR appears to be preferable to maximize EA under quasi-
 263 static compression [73]. A VCR value of 2.2 was recommended as the best for PU foams used in
 264 seat cushions [71].

265 To determine the effect of the material plasticity on energy dissipation of auxetic metal foams,
 266 numerical impact tests on foam finite element (FE) models have been carried out by Kumar *et al.*
 267 [74]. The plastic Poisson's ratio (the Poisson's ratio on the plastic stage ν_p should be close to zero
 268 to obtain the maximum energy dissipation.



269 **Figure. 10.** Summary of the recommended parametric combinations based on experiments in the
 270 literature of heating temperature, VCR and heating time (indicated by the number in blocks, measured in
 271 minutes) for different foam samples (indicated by the color of blocks) (Data obtained from [66-68, 70,
 272 71]).

274 PU foam samples were compressed using hydro-static pressure before being placed into the
 275 mold in the work of Najarian *et al.* [48], so the value of the pressure is also a critical parameter
 276 during in the conversion process in the work. In order to obtain foam samples with the best auxeticity
 277 and stiffness, a grey relational analysis (GRA) was proposed in the paper to control the influential
 278 parameters *viz.* temperature, pressure and time. The optimal combination of parameters involved

279 the values of 140 °C for the annealing temperature, 40 bar for pressure and 20 min for heating time.
280 Duncan *et al.* [55] recently investigated the effect of steam conversion on the cellular structure,
281 Young's modulus and negative Poisson's ratio of closed-cell LDPE foams. The formation of cells
282 with re-entrant shape tended to increase with the duration of steam conversion. Surprisingly, large
283 foam samples in the fabrication shrank more evenly than small ones, indicating this methodology is
284 a feasible way to fabricate large foam specimens.

285 Though lots of investigations have been conducted and the conclusions include detailed
286 parametric combinations to manufacture optimal auxetic foams, the recommended combinations are
287 regarded as reference to further experiments due to the variation of foam samples (such as chemical
288 constituents and sample size) and randomness of manufacturing condition (such as room
289 temperature for cooling). The size of foam samples, in fact, is of significance in the manufacturing
290 consisting in heating process and should be taken into further consideration.

291 **3. Micro-structure and deformation mechanisms in auxetic foams**

292 Solid understanding of micro-structure and deformation mechanism in auxetic foams is not
293 only the foundation to explore efficient manufacturing methodologies, but also desirable to create
294 valid foam models using in numerical analysis and finite element modeling (FEA). Such models
295 could also be utilized for inspiring auxetic structural design.

296 ***3.1 Re-entrant polyhedron models of auxetic foams***

297 The first step in developing micromechanical models for these foams is to define the geometry
298 of the original and converted foam cells. The internal pressure and squeezing of neighbor cells or
299 surfaces during the foaming stage generate cells with multiple polyhedron shapes. Most of the
300 earliest studies on foam structures have been focused on simplified topological representations
301 involving faceted polyhedrons (**Figure. 11**). Lakes [15] is the first to present stereo photographs and
302 an idealized re-entrant unit cell structure for the auxetic foams, in which the ribs were bent and
303 protruded into the cells: an axial tensile load would cause the cell to unfold and expand laterally.
304 Later, Friis [30] developed the topology of the model further by using the Kelvin minimum area
305 tetrakaidecahedron consisting in a convex shape with eight curved hexagonal faces and six curved
306 square faces. However, the description of how conventional foam deforms was absent. Wei [75]
307 extended the lattice formulation of Warren and Kraynik [76] to represent polymeric networks via
308 three arms of equal length and one backbone all connected to one junction. The model could be
309 applied to both 2D and 3D cases. Choi *et al.* [77] proposed a novel 3D tetrakaidecahedron model
310 accompanied by a description of how it could assume a re-entrant structure. Doyoyo *et al.* [78]
311 presented a 3D auxetic structural lattice and verified that it could predict some mechanical properties
312 of previously published auxetic foam materials. Cham *et al.* [79] argued that the tetrakaidecahedron
313 model is not adequate to consider anisotropic foams with a preferential rise direction during foaming
314 or thermoforming, and therefore introduced a more generally accepted dodecahedron model.

3D models







	Conventional	Auxetic	Reference
(a)			[18,78]
(b)			[30,77]
(c)			[79]

Figure. 11. 3D polyhedral models of auxetic foams proposed in literature: (a) Idealized re-entrant unit cell structure, original foam structure is not given in the paper [18,78], (b) Kelvin minimum area tetrakaidecahedron model [30,77] and (c) Dodecahedron model [79].

3.2 2D models of auxetic foams

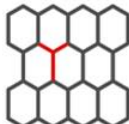
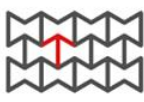
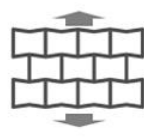


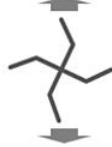
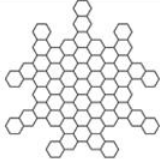

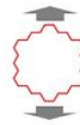


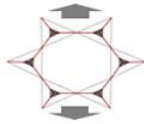
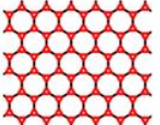
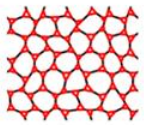
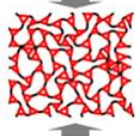
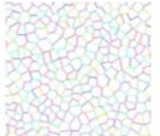


Various 2D models have also been developed to provide a more simple explanation of potential deformation mechanisms occurring inside auxetic foams when subjected to loading (**Figure. 12**). The 2D lattices derived from 3D configurations could be also helpful to inspire the design of general 2D auxetic materials. Early studies considered the auxetic structure of the foam as derived from the hexagonal configuration lattice [42, 80, 81] and modified those centrosymmetric topologies into auxetic ones [42, 80-83]. In those models the auxetic behaviour requires the deformation of the foam ribs from “Y” shape to “arrow-head” joints (i.e., the re-entrant structure). Another 2D model named “missing rib” model was proposed by Smith *et al.* [49]. This model could explain the auxeticity and the strain-dependent Poisson’s ratio behaviour by further fitting some of its parameters to experimental data. Further modifications of the missing rib model were introduced by Gaspar *et al.* [84] and Lim *et al.* [85], with improved accuracy in terms of the prediction of the Poisson’s ratio of the auxetic foams. However, Gaspar *et al.* [86] also noted that missing ribs are actually existing in real auxetic foams, but their fraction over the total of the foam ribs is quite small and the dominant deformation within the auxetic cells is still the bending of straight ribs.

In 2005, Grima [87] proposed a system based on rotating components linked by rigid or flexible

335 joints / ribs to explain the deformation mechanism in auxetic foams when compressed. The rigid
336 joints inside the foams could be simplified into triangles [87-89] . Pozniak *et al.* [90] have developed
337 two 2D models of auxetic foams (Y and \triangle models). These two simple disordered structures could
338 predict well the deformation of foams under compression. An extended model was proposed by
339 Chetcuti *et al.* [89] that took into account the amount of material at the joints and the deformation
340 of the joints themselves, this model allowed a set of more plausible predictions of the Poisson's
341 ratio values. Similar disordered structure for simulating auxetic foams is the 2D random cellular
342 solid model proposed by Li *et al.* [91]. Regular 2D Voronoi model was given a irregularity of 0.45
343 and then modified by a process of merging and removing to correspond with the geometric shape
344 of experimental auxetic foams. Alderson *et al.* [92] proposed three 2D topologies based on the
345 observation of micrographs of auxetic foams to illustrate the effects of uni-axial, bi-axial and tri-
346 axial compression on the pore structure. Simular works have been carried out by Bianchi *et al.* [46]
347 for invastigating the deformation mechanism of converted foam samples fabricated by "half mould"
348 process.

349 Similarly to 3D models, the 2D models of auxetic foams allow to predict the auxeticity and
350 the mechanical of the porous materials. The deformation mechanisms predicted by these models
351 could also inspire future works in designing novel auxetic structures.

2D models

	Conventional	Auxetic	Deformation	Reference
(a)				[43,80-83]
(b)				[48]
(c)				[85]
(d)				[87-89]
(e)				[90]
(f)				[91]

352 **Figure. 12.** 2D models of auxetic foams proposed in literature: (a) the transformation of “Y”
 353 shape joints to “arrow head” joints [43,80-83], (b) chiral structure produced by “Missing
 354 ribs”(broken ribs caused by compression, melt ribs caused by heating process or removed ribs
 355 caused by acetone) [48], (c) modified re-entrant “missing rib” model based on hexagonal foam cells
 356 [85], (d) regarding the joints as triangle shape, and the deformation based on the rotating of joints
 357 which resulting the re-entrance of foam ribs [87-89], and disordered foam structures based on (e)
 358 rotational joints model [90] and f) 2D Voronoi model [91].
 359

360 **3.3 Microphotographs and FE models of auxetic foams**

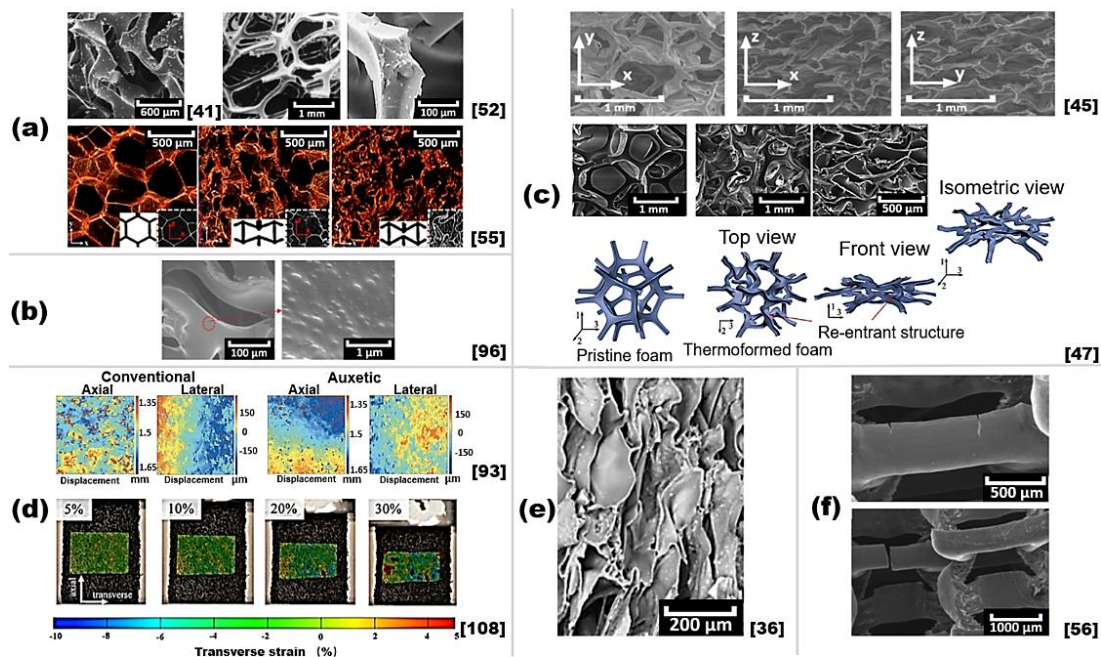
361 The use of various imaging technologies such as digital image correlation (DIC), X-ray
 362 scattering, computed tomographic (CT) and scanning electron microscope (SEM) allows to identify
 363 the internal structure and deformation mechanism of auxetic foams (**Figure. 13**). Alderson *et al.* [34]
 364 observed that the auxetic behaviour of auxetic thin flat pads fabricated by uni-axial compression
 365 was due to a through-the-thickness crumpling of the cells, and evidence for the existence of the
 366 equivalent of rotation joints has been provided by X-ray microtomography [93, 94]. SEM has also
 367 allowed to observe bending, stretching, hinging and obvious rotations of elements of the foam pores

368 during compression [73], indicating the presence of an heterogeneous deformation during the
 369 compression of foams. Similar studies based on CT techniques have been carried out by Elliott *et al.*
 370 *al.* [95], who also observed the presence of bending and entirely collapsed layers of cells and struts
 371 impinging on each other during compression.

372 SAN particles (mentioned in 2.2, the utilizing of CO₂) were observed in PU foams by Li *et al.*
 373 [96], and this nanoparticle compound provided a likely explanation of the annealing temperature
 374 mechanism within the fabrication of the foams. The finding of the consisting of SAN copolymers
 375 also promotes further investigations on auxetic foam manufacturing modifying.

376 The imaging technologies mentioned above have also allowed to identify strong local
 377 heterogeneities of open-cell PU foams [85, 86, 97, 98], anisotropic behaviour in closed-cell PU
 378 foams [39, 97, 99] and open-cell PU foams [46, 47], difference in distribution of reduction in size
 379 of cells in the closed-cell PE foam [36] and defects of the foams fabricated using 3D print [56].
 380 Recently, Pashineet *et al.* [100] interpreted the deformation of auxetic foams as a directed aging
 381 process, under which foam samples develop along an expected direction at larger scale like network
 382 bonds, rather than at microscopic one.

Microphotographs

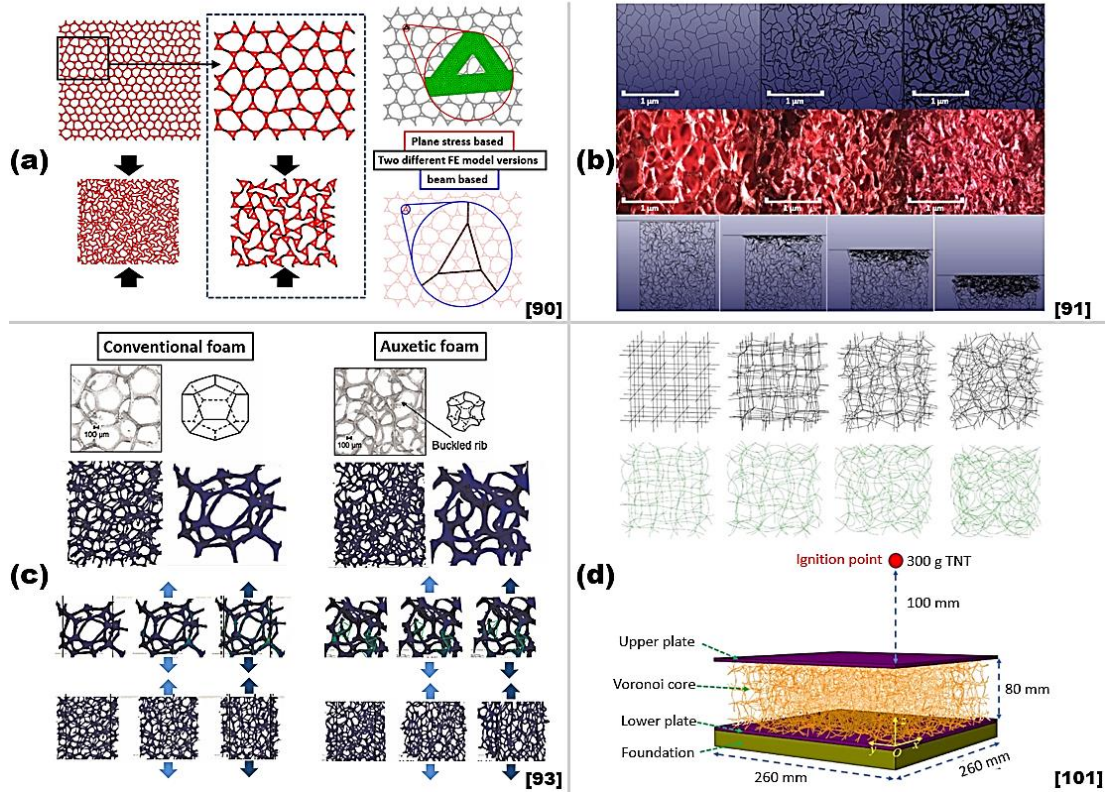


383
 384 **Figure. 13.** Images of the microstructure of auxetic foams in literature: (a) Observations of
 385 bending, stretching, hinging and obvious rotating during compression [52,55], (b) SAN particles which
 386 provided a likely explanation of the annealing temperature mechanism within the fabrication of the
 387 foams [96], (c) anisotropic behavior in auxetic foams [45,47], (d) local heterogeneities in auxetic foams
 388 [108], (e) difference in shrank distribution in the closed-cell PE foam during the steam treatment [36]
 389 and (f) defctions of the foams fabricated by 3D print technology [56].

390 The imaging technologies allow the identification of foam structures and their deformation
 391 mechanisms. Micrographs and 3D images obtained by using CT could also be used to develop solid

392 models of the foam skeletons and microstructures, and be transferred to the finite element analysis
393 (FEA) software for simulating the mechanics and deformation mechanisms of these foams at much
394 higher fidelity (**Figure. 14**). Two 3D region of interest models were crated and transformed into FE
395 models by McDonald *et al.* [93]. The local rib interactions and goble displacement of foam
396 samples can be faithfully represented by followed FEA process, providing confirmation to the
397 mechanisms observed in the experiments and greater details occurred in foam samples under applied
398 loadings. The above-mentioned 2D auxetic models that proposed by Pozniak *et al.* [90] and Li *et al.*
399 [91] can also be built in FEA softwares. Pozniak *et al.* proposed two approaches for simulating the
400 structures they proposed : the plane stress based and the beam based approach. These two
401 approaches are valid to simulate proposed structures, however, in consideration of both calculation
402 speed and simulating accuracy, the latter approach was recommended as the better one. As for the
403 works of Li *et al.*, different area compression ratios A_r was adopted in structural design to correspond
404 with the different VCRs that adopted in actual copper foams according to ref.[33]. The excellent
405 agreement achieved between FEA and experimental observations shows that these irregular
406 structures can highly simulate the deformation of actual auxetic foam samples. Some mechanical
407 properties such as the Poisson's ratio behavior and EA capacity can also be predicted to some extent
408 by similation results of these structures. In order to investigate the blast resistance of auxetic
409 structures, Li *et al.* [101] built a series of 3D isotropic auxetic foam core in FEA software by using
410 random Voronoi structures. The Poisson's ratio varies from positive to negative by changing the
411 randomness and tri-axial compression ratio of the structures, providing a feasible methodology to
412 build auxetic FE models.

Finite element models



413 **Figure. 14.** FE models of auxetic foams in literature: (a) Two different FE model versions (plane
 414 stress based and beam based) for the proposed disordered auxetic structures [90], (b) 2D random
 415 cellular solid models based on a modified Voronoi tessellation technique for simulating the
 416 compression of copper foam [91], (c) microstructurally faithful FE models created from the
 417 reconstructed 3D tomography data [93], and (d) 3D isotropic auxetic foam core for blast resistance in
 418 FEA software by using random Voronoi structures [101], the structures can be generated by using
 419 different randomness (upper black ones) and tri-axial compression ratio (lower green ones).
 420

4. Mechanical properties of auxetic foams

422 The most particular property of auxetic foams is the possession of negative Poisson's ratio ν ,
 423 which is directly related, according to the classical theory of elasticity [102], to the Young's modulus
 424 E , the bulk modulus K (or resistance to changes to volume due to the application of a hydrostatic
 425 pressure) and the shear modulus G (or resistance to shear surface forces) in an isotropic material.
 426 The variation of the Poisson's ratio can significantly affect the mechanical behavior of the material.
 427 In an isotropic material with a constant E , if ν approaches - 1, the shear modulus G theoretically
 428 approaches to infinity, i.e., such material could be easily compressed but hard to shear.

$$429 \quad G = \frac{E}{2(1 + \nu)} \quad (1)$$

$$430 \quad K = \frac{E}{3(1 - 2\nu)} \quad (2)$$

$$431 \quad E = \frac{9KG}{(3K + G)} \quad (3)$$

432

$$\nu = \frac{3K - 2G}{2(3K + G)} \quad (4)$$

433

434

435

436

437

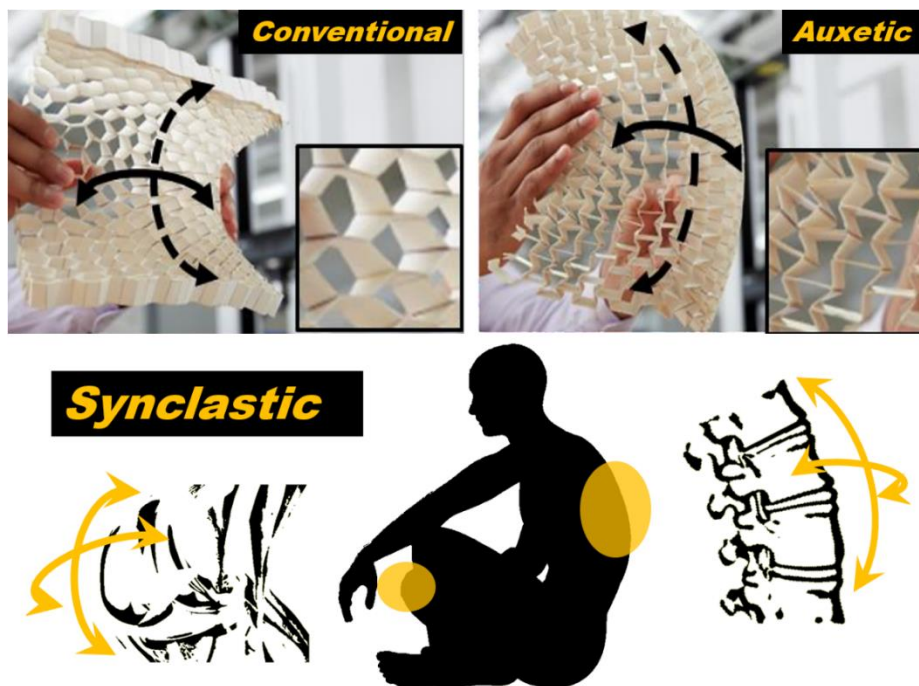
438

439

440

441

Though auxetic foams are highly anisotropic [15, 19, 97, 99, 103-105] and other relations between engineering constants need to be applied within the framework of classical elasticity to predict the behavior of anisotropic auxetics [106-108], auxetic foams show indeed better indentation shear resistance though the Young's modulus is smaller (lower E) than conventional ones [19, 31, 38, 45, 83, 108, 109]. The shear modulus in quasi-isotropic auxetic open cell foams can be well approximated using the formulas related to classical isotropic elasticity [110], but the shear stiffness of transverse isotropic auxetic foams has a different behavior [111]. The shear moduli vary between 10 - 38 kPa measured with a pure shear test [110] and 30 - 60 kPa via 3 point / 4 point bending tests [111], with the latter measurements taken at higher strain rates.



442

443

444

445

446

447

448

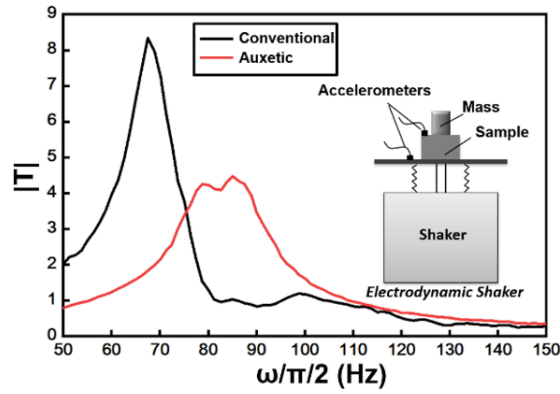
449

450

451

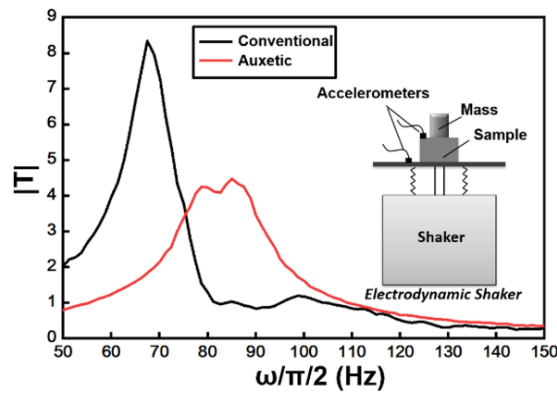
Figure. 15. Synclastic (dome-shaped) curvature behavior of materials with a negative Poisson's ratio, and drawing pictures present the ergonomic of this behavior (Images courtesy Andrew Alderson).

In terms of foam applications, the mechanical properties of stiffness (deformation resistance), hardness (indentation resistance) and toughness (fracture resistance) are very important. Auxetic foams also possess peculiar characteristics like the synclastic (dome-shaped) curvature (**Figure. 15**) [15, 19], reduction of vibration transmissibility (**Figure. 16**) [112], acoustic absorption (**Figure. 17**) [108, 112-118] and variable permeability (**Figure. 18**) [82, 119] Auxetic foams could also be made reversible, which means that the foams can be converted to their original state by a reforming process, i.e., they exhibit shape memory. (**Figure. 19**) [36, 43, 44, 54, 67, 74, 120, 121].



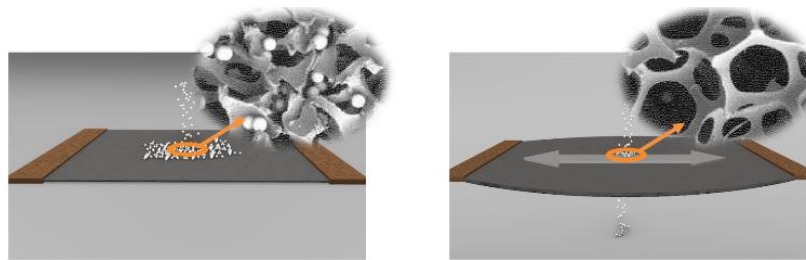
452
453
454
455

Figure. 16. Comparison between the vibration transmissibility ($|T|$) of conventional and auxetic foams between 49 and 150 Hz at low amplitude vibrations via electrodynamic shaker excitations (Data replotted from [112]).



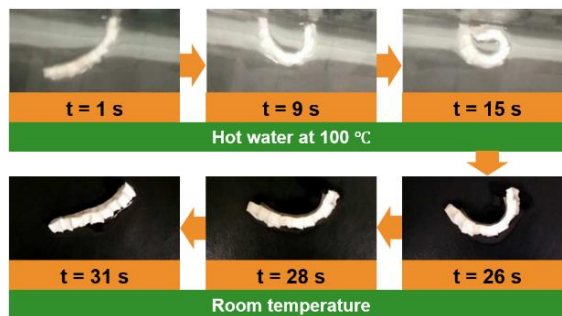
456
457
458
459

Figure. 17. Comparison of the frequency-dependent acoustic absorption between conventional and auxetic foams measured via acoustic impedance tube (Data replotted from [112]).



460
461
462

Figure. 18. Illustration of permeability tests with glass beads with auxetic foams, the foam pores can be enlarged by stretching (Images from [119]).



463
464

Figure. 19. Shape memory behavior of auxetic PE foam (Adopted from [36]).

4.1 Stiffness

The stiffness k is a parameter used to assess the deformation resistance offered by an elastic body:

$$k = \frac{F}{\Delta l} \quad (5)$$

Where F is the force applied on the body and Δl is the resulting deformation of the body. The stiffness and its evolution could significantly affect the EA and peak force under specific sets of loadings.

The stiffness of auxetic foams is in general lower than their conventional counterpart at lower compression strains (**Figure. 20**) [30]. Chan and Evans [122] thought conventional foams need to overcome the stiffness of their hexagonal pristine structure before the ribs become bent, whereas the ribs of auxetic foams are already bent when testing. Such phenomenon was also found by Bhullar [123], and the paper proposed that the lower stiffness at small strains could be beneficial to biomedical implants.

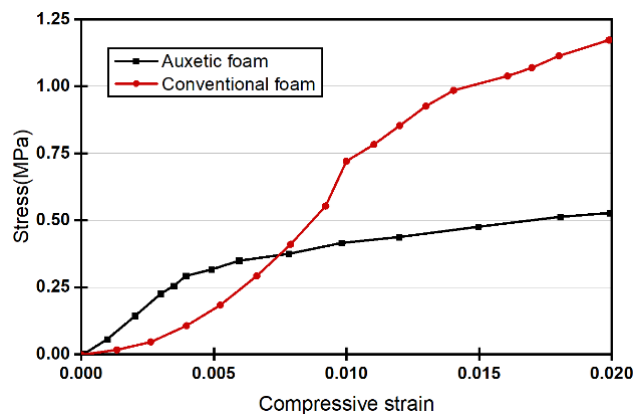
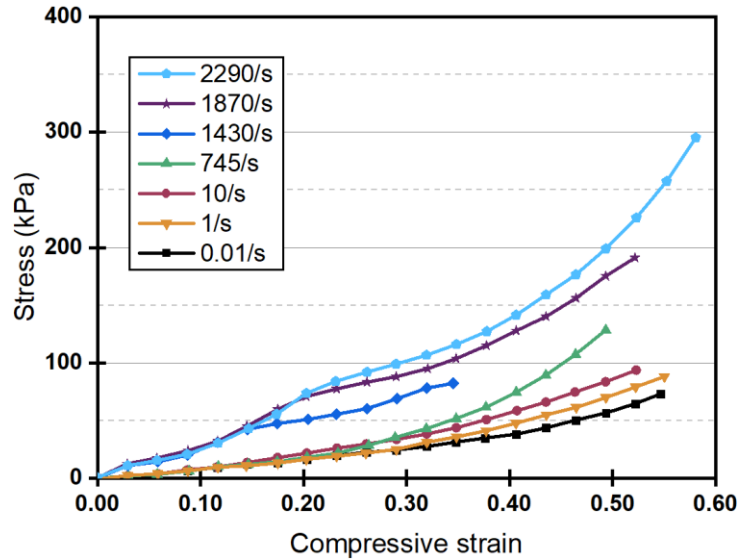


Figure. 20. Initial part of compressive strain-stress curves of auxetic foam and conventional foams (Data replotted from [30]).

As the compression increases, auxetic foams shrink laterally due to their unique re-entrant structure, making the density and stiffness increase significantly. Such phenomenon can be seen in other auxetic structures and nowadays the stiffness control [124] during the loading process has become a research point. On the contrary, conventional ones expand laterally and the density and stiffness in general feature more limited changes. Auxetic foams will therefore tend to be denser and stiffer than conventional ones at higher compression strains. A lower stiffness of auxetic foams could only be observed in a very small strain and hardly exists in samples having small scale pores. Foam materials are widely used to undergo large deformation, so the lower stiffness in the very beginning part could be negligible in most applications, although stiffness at small strain is also a parameter that affect the static indentation of foams and the comfort provided in cushioning. The stiffness of auxetic foams is sensitive to strain rate: the higher the strain rate be applied, the stronger the stiffening effect [20, 125] (**Figure. 21**).



493
494 **Figure. 21.** Compressive strain-stress curves of auxetic PU foam at various strain rates (Data replotted
495 from [20]).

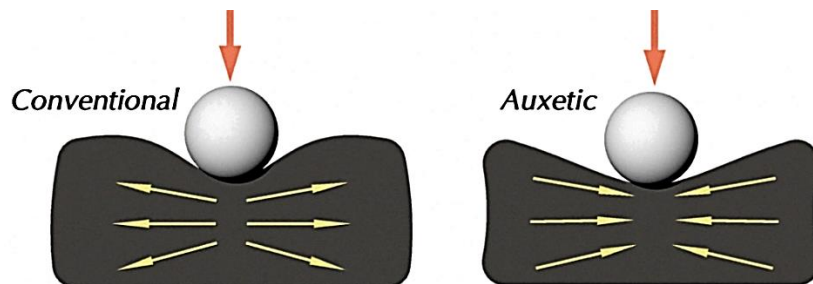
496 **4.2 Hardness**

497 The hardness of foam materials is one of the representative parameters to evaluate their
498 indentation resistance. The increased hardness of auxetic foams could be also predicted from the
499 perspective of the classical elasticity theory, the relationship of hardness (H) and Poisson's ratio (ν)
500 is given by:

501
$$H \propto \left[\frac{E}{(1 - \nu^2)} \right]^\gamma \quad (6)$$

502 Where E is the Young's modulus, γ is 1 under uniform load or $2/3$ under concentrated load.
503 When the ν approaches -1, the stiffness approaches to infinity.

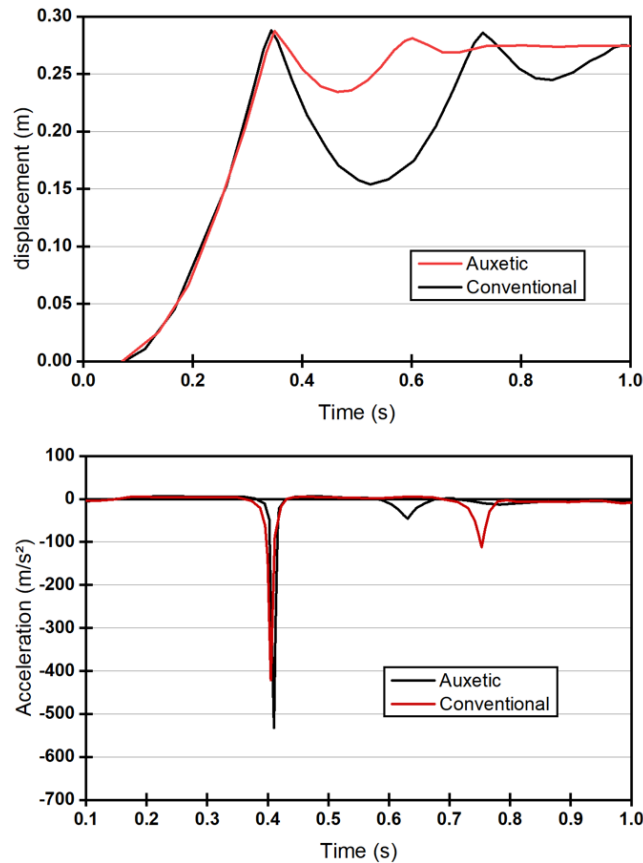
504 Superior hardness of structures with a negative Poisson's ratio was reported in previous
505 experiments [126-128]. Auxetic materials feature a unique type of deformation under indentation:
506 the material around the loading area will tend to concentrate towards the impact point, causing a
507 significant increase of local hardness. On the contrary, materials with positive Poisson's ratio would
508 expand outwards from the impact point in similar loading conditions, making indentation easier
509 (**Figure. 22**). This indentation resistance behavior has also been experimentally observed in auxetic
510 foams [45, 47, 117, 122, 129-135].



511 **Figure. 22.** Inner reactions under indentation of conventional (left) and auxetic foam (right).
512

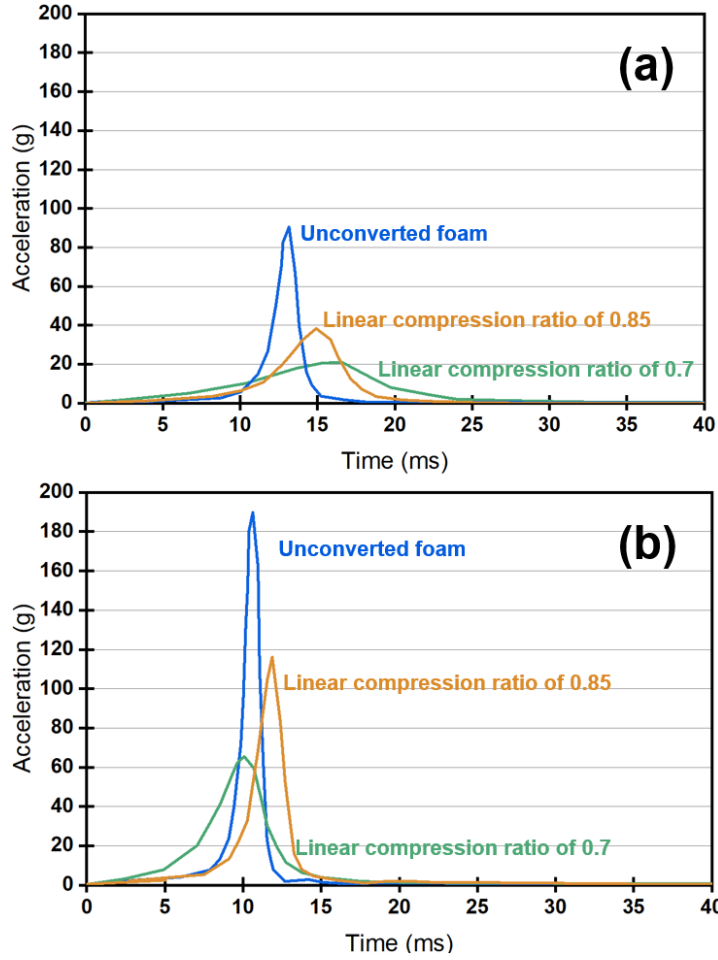
513 Lisiecki *et al.* [51] argued that auxetic foams produced via the mechanic-chemic-thermal

514 process are not suitable for impact mitigation due to their tendency of becoming denser under
515 indentation or compression. Those authors performed quasistatic and drop tests, and indicated the
516 higher deceleration and smaller impact hammer displacements at an equivalent static pressure of
517 12.3 kPa as evidence for their conclusions (**Figure. 23**).



518 **Figure. 23.** Time histories of the hammer displacement (top) and acceleration (low) on auxetic and
519 conventional foams for an equivalent static pressure of 19.6 kPa (Data replotted from [51]).

520
521 Soft foams may however bottom out under indentation [112, 136], slightly higher stiffness of
522 auxetic foams may therefore provide more comfort as a cushion. Lakes and Lowe [71] noted that
523 the volumetric compression ratio (or the final density) is critical to obtain an optimal performance
524 under indentation in auxetic foams. Measurements of pressure distributions on PU foam cushions
525 were performed by those Authors, and the results showed that the re-entrant foam at densities
526 between 0.032 and 0.064 g/cm³ performed better (i.e., lower maximum seating pressure) than
527 conventional foam samples at comparable density. The auxetic foam material also wraps around the
528 indenter under indentation, which provides a more uniform stress distribution and a reduced
529 pressure concentration [71, 136, 137]. Further studies of Allen *et al.* [137] and Duncan *et al.* [138]
530 showed that the peak accelerations (synchronized with the maximum deformation) of flat indentors
531 used in drop tests on thermoformed-mechanical auxetic foams are smaller than in conventional ones
532 under low-kinetic energy impact conditions. This indicated that those auxetic foams are promising
533 for applications like cushions and pads (**Figure. 24**).



534
 535 **Figure. 24.** Time histories of the acceleration for the flat indenter used in drop tests on R45FR foam at
 536 (a) 2 J and (b) 4 J of kinetic energy (Data replotted from [137]).

537 **4.3 Toughness**

538 Toughness indicates the ability of a material to resist fracture, and it is also a parameter adopted
 539 in crashworthiness designs [113, 139-141]. Toughness is in general critical for materials used in
 540 packaging and protection and it is measured by the area underneath the load-displacement or strain-
 541 stress curve. That area is also the value EA, while the specific energy absorption (SEA) indicates
 542 the energy absorbed per unit mass of the structure. These two parameters could be calculated as
 543 follows [142, 143]:

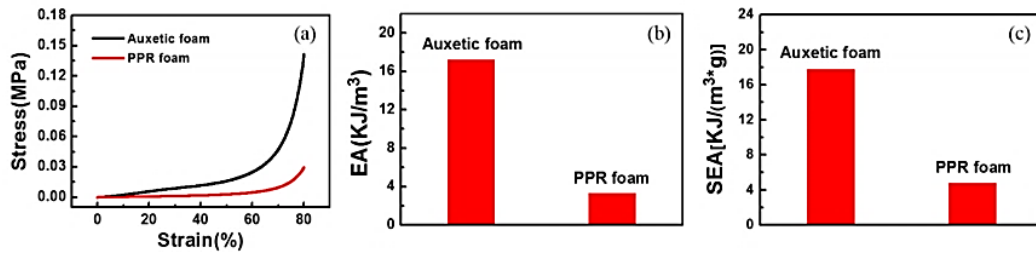
544
$$EA(d) = \int_0^d F(x) dx \quad (7)$$

545
$$SEA(d) = \frac{EA(d)}{m} \quad (8)$$

546 In those equations d is the crushing distance, F is the crushing force and m is the mass of the
 547 structure.

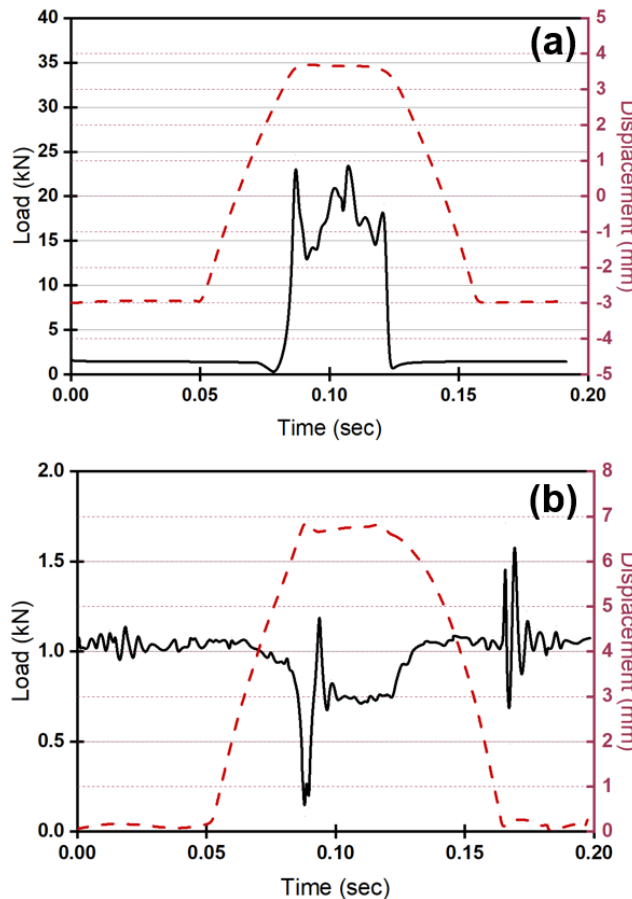
548 The parameters EA and SEA can be determined from quasi-static mechanical tests. Under
 549 quasi-static loading, auxetic foams absorb more energy than their conventional counterparts [40, 51,
 550 54, 69, 101, 131, 132, 144-148]. A comparison of compression properties between auxetic foams

551 and PPR (Positive Poisson's ratio) foams in ref. [54] is presented below as an example in **Figure.**
 552 **25.**



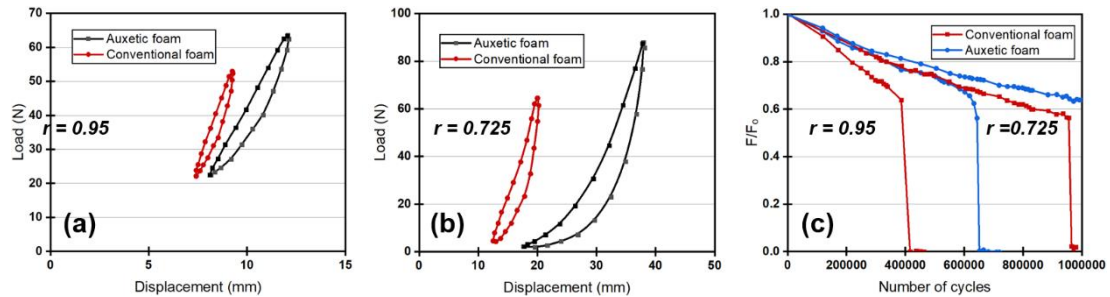
553 **Figure. 25.** Compression of auxetic and the PPR foams: (a) compressive stress-strain curve, (b) EA
 554 values for the auxetic and the PPR foams and (c) SEA for the auxetic and the PPR foams [54].
 555

556 Mohsenizadeh and his group tested a series of auxetic foam-filled square tubes under both
 557 quasi-static and crushing tests with loading velocity of 1.5 m/s [139-141]. The EA value of the tube
 558 increases as the auxeticity of foam filler increases. The works of Scarpa *et al.* [80, 113] recorded the
 559 time histories of load and displacement in auxetic and conventional foams under high strain rate
 560 compression (**Figure. 26**). The time histories related to the auxetic foam demonstrated a better
 561 consistency, indicating a significantly improved resilience of the auxetic foam compared to the
 562 pristine conventional foam samples.



563 **Figure. 26.** Time histories of displacements and loads for (a) auxetic and (b) conventional foams under
 564 dynamic crushing loading conditions (cam plastometer) at 15 s^{-1} . The full curve represents the force
 565 history and the broken curve represents the displacement history (Data replotted from [113]).
 566

567 A series of fatigue tests were carried out by Bezazi and Scarpa [131, 149] to investigate the
 568 toughness, stiffness loss and damping capacity of auxetic foams under cyclic loading (**Figure. 27**).
 569 In those studies, the maximum load F was recorded as a function of the number of cycles N and
 570 normalized by the maximum load F_0 obtained during the first cycle. The loading level r was defined
 571 as the ratio between the maximum displacement at a particular level to the displacement at failure.
 572 A larger energy dissipation was observed in the displacement-load curve of the first cycle and the
 573 auxetic samples show a lower stiffness degradation (rigidity loss) (F / F_0) after a large number of
 574 cycles compared to the parent conventional ones.



575
 576 **Figure. 27.** Direct comparison between first cycle hysteresis loops for auxetic and conventional foams
 577 at different loading levels of (a) $r = 0.95$ and (b) $r = 0.75$; (c) Stiffness degradation versus number of
 578 cycles for the two types of foams at different loading levels: $r = 0.95$; $r = 0.725$ (Data replotted from
 579 [131]).

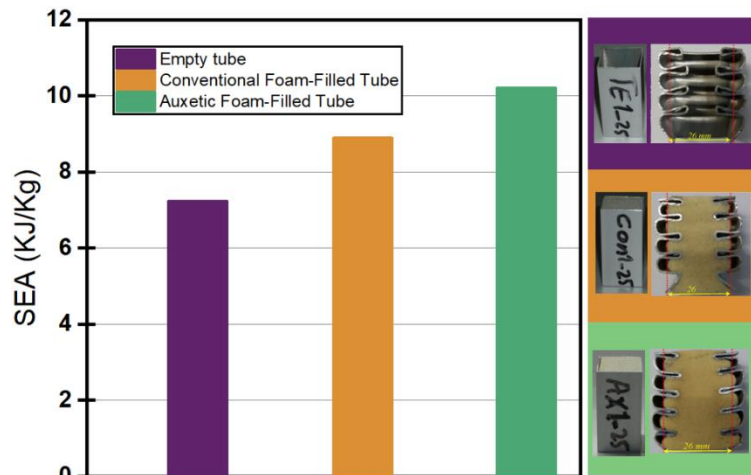
580 Another less documented but important parameter is the fracture toughness evaluated by Choi
 581 and Lakes [31] in auxetic copper foams, with significant improvements compared to the
 582 conventional copper foam version. Although those enhanced properties in fracture are promising in
 583 terms of the load-bearing applications, to the best knowledge of the authors of this review, no other
 584 work has focused on the fracture toughness of auxetics yet.

585 5. Applications of auxetic foams

586 Auxetic foams are in essence transformed from traditional porous materials. The
 587 transformation leads to a set of very desirable properties that conventional foams do not possess. It
 588 is therefore reasonable to consider auxetic foams either as a replacement of conventional porous
 589 materials, or as the basis of completely new designs to exploit their ad-hoc properties. Foam
 590 materials are commonly used as fillers for cushion and auxetic foams, compared to conventional
 591 ones, may further improve comfort and reduce the risk of pressure sores because of their EA [51]
 592 and pressure reduction [71, 136, 150]. These superior properties are also highly attractive for
 593 protective equipment in sports applications such as pads or mats [51, 71, 136], gloves [144], helmets
 594 [132, 151], sports shoes [132] and snow-sport safety devices (body armour and crash barrier) [145].

595 Several thin-walled tubes with auxetic foam core have been designed by Mohsenizadeh et al.
 596 [140, 141, 152]. Compared to the control group made with conventional foam, the compression
 597 induced shrinkage (density increasing) of the auxetic foam core provides enhanced EA and
 598 crashworthiness (**Figure. 28**). Recently, Zhang et al. proposed a series of auxetic tubes with superior
 599 mechanical properties [153, 154], compared with the ordinary tubes as the above-mentioned ones,

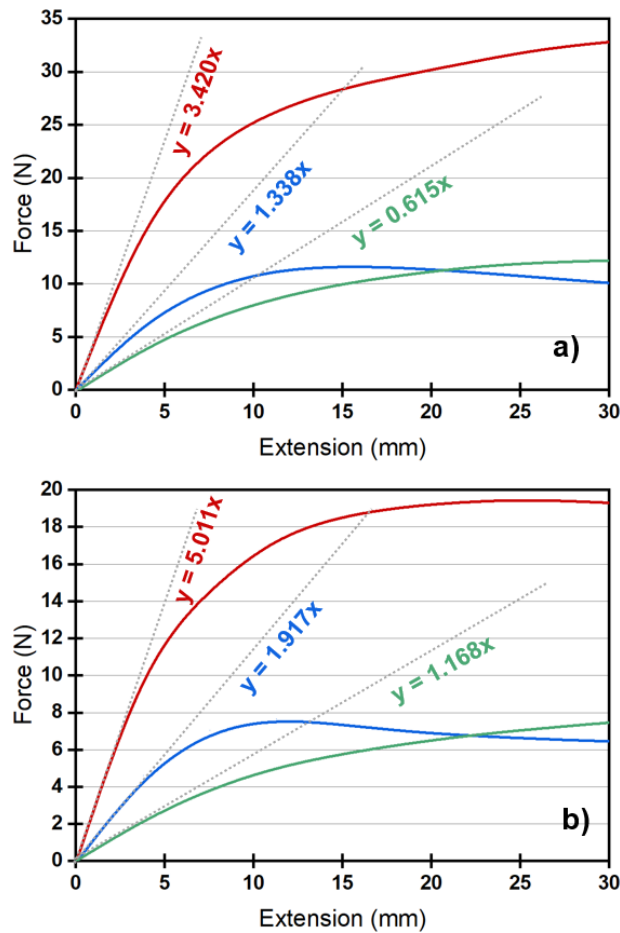
600 such novel auxetic tubes could further enhance the mechanical performance of auxetic foam-filled
601 tubular structures.



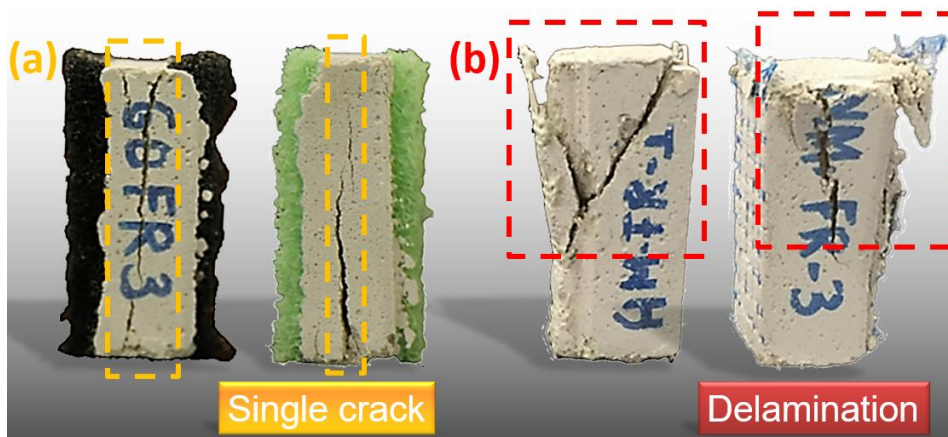
602
603 **Figure. 28.** SEA and sections of foam-filled tubes (Adapted from [153]).

604 Sandwich composite beams with auxetic foam core could bear large loading (high shear stress)
605 under large deformations [111] and possess significant mechanical impedance with an interesting
606 zero stiffness behavior [155] (**Figure. 29**). Depending on the type of application and loading, auxetic
607 foams could be used to tailor the performance and the overall weight of the structural sandwich
608 panel in which they are embedded. Zahra *et al.* [156] have described the manufacturing and
609 characterization of cementitious polymer mortar-auxetic foam composites and showed that the
610 embedding of the auxetic foam could avoid delamination and brittleness of the cement (**Figure. 30**).
611 The unique deformation under compression (material concentration at compression area (**Figure.**
612 **22**)) endows auxetic foam with enhanced resistance for fracture. Such outstanding performances are
613 potential in the engineering field. Except for axial compression, it is also worth researching to test
614 auxetic structures under complicated loading conditions.

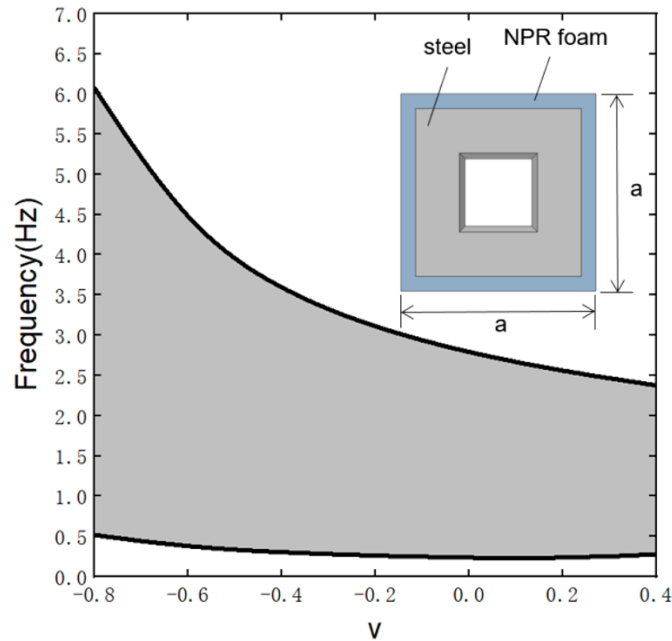
615 Recent progress in seismic metamaterial was reported by Huang *et al.* [157], a series of
616 numerical simulations certified the positive function of auxetic foams as the shell to attenuate Lamb
617 wave, realizing the generating of ultra-low frequency bandgap (**Figure. 31**). Their work is
618 significant to researchers who are devoted to the wave or sound isolated function of auxetic foams.
619 Such lightweight functional material is also promising in civil engineering and disaster prevention
620 and mitigation.



621
 622 **Figure. 29.** Force versus central deflection for a) 3-point and b) 4-point bending test on sandwich
 623 panels with different foam cores. Green, auxetic; blue, conventional thin; red, conventional thick. The
 624 slope of dashed lines represents tangent stiffness of the proposed foam cores (Data replotted from
 625 [111]).



626
 627 **Figure. 30.** Cracking characteristics of (a) cementitious polymer mortar - auxetic foam composites
 628 and (b) cementitious polymer mortar-PPR fibreglass mesh composites (Adapted from [156]).



629 **Figure. 31.** The novel seismic metamaterial based on auxetic foam and the effect of Poisson's
 630 ratio of auxetic foam on the first complete bandgap (Adapted from [157]).
 631

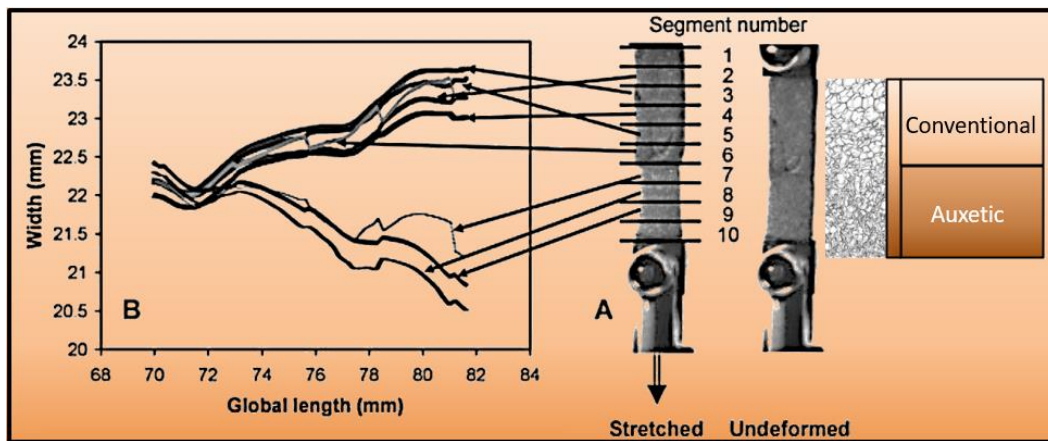
632 For investigating and utilizing the behavior of auxetic foams under torsion, semi-auxetic rods
 633 have been designed by Lim [158]. This novel design of rods produces unique mechanical behaviors
 634 under torsion for potential use as smart structures with different responses under multivariate
 635 loading. Concentric auxetic-conventional foam rods with high modulus adhesive at the interface
 636 have been modeled using an analytical approach to investigate the effect of the adhesive on the
 637 overall auxeticity of the system [159]. As for bending condition, where auxetic materials present the
 638 characteristics of synclastic curvature, Mohanraj *et al.* [150] designed a hybrid composite support
 639 for people with multiple sclerosis, consisting of an auxetic open cell foam liner and curved
 640 thermoplastic plates with rhomboidal perforations. Different types of material substrates allowed in
 641 this design can contribute to reducing the capital costs of development and increase the life cycle of
 642 the products for these particular biomedical applications. Synclastic curvature is an ergonomic
 643 deformation mode to perfectly stick a human's head, dorsum and joints (**Figure. 15**). In that, the
 644 more uniform stress distribution provided by shape fitting could be also used as soft tissue implants
 645 in cartilage articulations and meniscus repair for knee prosthetics [123].

646 Honeycomb membranes with conventional and re-entrant cell geometries have been
 647 successfully fabricated and tested by Alderson *et al.* [160], re-entrant samples show an enhanced
 648 functional performance compared to conventional (hexagonal ones) ones for glass chromatography
 649 beads in applications related to filtration systems. Inspired by this unique property of auxetic
 650 structures, a series of studies on auxetic foams were performed by the group of Alderson [82, 119].
 651 A variation of the pressure-drop and transport properties was also observed in auxetic foams, making
 652 the negative Poisson's ratio porous material appealing for sieving of beads of uniform diameter and
 653 air pressure-drop applications (**Figure. 18**). The dramatic change of pore size that auxetic open cell
 654 foams exhibit under mechanical loading (compact re-entrant pore to expanded hexagonal pore under

655 stretching) can be useful to compensate the increase in pressure-drop which arises due to increased
656 filter fouling, flushing or altering the response of a filter or catalyst structure.

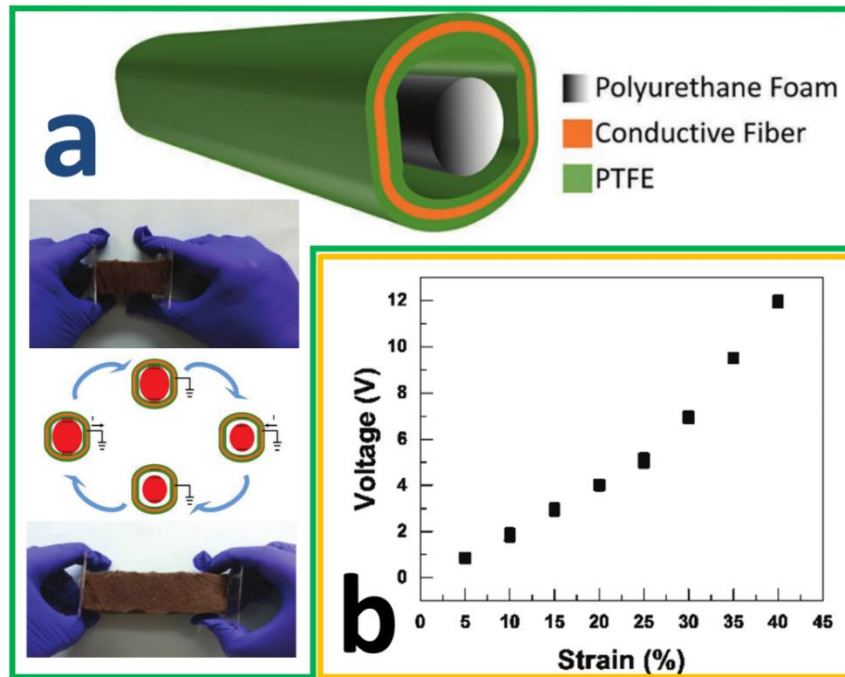
657 The large displacements given by the auxetic behaviour for a given applied load have been also
658 highlighted by Scarpa *et al.* [113], and a proposal for using auxetic foams to enhance self-sensing
659 structural components was there presented. This large deformation feature of auxetic foams was
660 used to develop variable stiffness and shape hybrid negative Poisson's ratio PU-PE foams saturated
661 with magnetorheological fluids (MRFs). These smart foam systems have shown tunability of the
662 stiffness and magnetostrictive effects (up to 4 times stiffness increase by applying 0.2 T of magnetic
663 field) [161, 162] and tunability of the electromagnetic and acoustic absorption of surface-coated
664 MRF foams [115]. Auxetic open cell PU-PE foams seeded with carbonyl particles and
665 magnetorheological fluids have also shown an increase of the acoustic absorption by a factor of ~ 7
666 compared to the pristine foam within the 1 kHz - 2.5 kHz bandwidth and the presence of a peak
667 absorption of ~ 1 with the MRF that could be shifted by almost 500 Hz when applying magnetic
668 fields between 0.1 T and 0.2 T [114].

669 As a soft material with significant lateral deformation under longitudinal loadings, auxetic
670 foams are great candidates to serve as sensitive movement sensors. In 2013, Alderson *et al.* [163]
671 introduced the term "piezomorphic" to describe mechanically-triggered shape change materials and
672 proposed an elastic-gradient piezomorphic material (**Figure. 32**) made from PU foam and micro
673 porous polymer (ex-PTFE). The piezomorphic material possesses both negative and positive
674 Poisson's ratio regions and show a dramatic shape change triggered by the application of global and
675 local stresses.



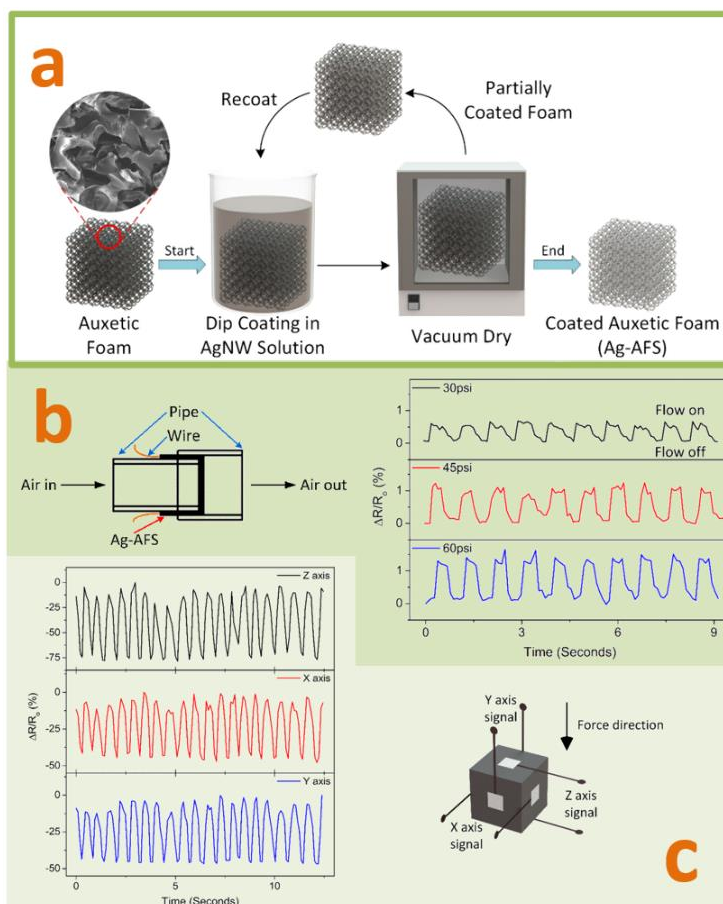
676
677 **Figure. 32.** Global length-width curves of different parts related to the elastic-gradient
678 piezomorphic material (Adapted from [164]).

679 The piezomorphic behaviour could also be exploited to use auxetic foams as platforms to build
680 sensors. The first contact-mode triboelectric self-powered strain sensor using an auxetic PU foam
681 (**Figure. 33**) has been fabricated by Zhang *et al.* [164]. This sensor can be used in human body
682 monitoring systems, self-powered scales to measure weight or in seat belts to measure the body
683 movements on a car seat.



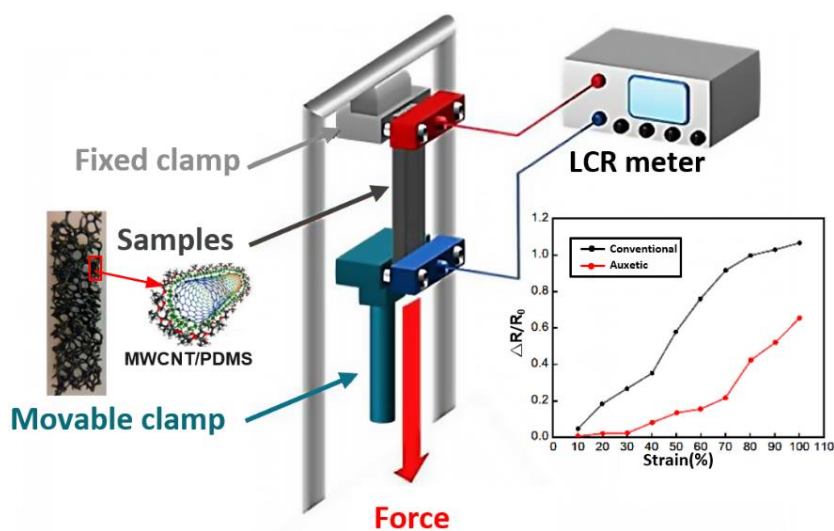
684
685 **Figure. 33.** (a) Schematics and (b) voltages under different tensile strains of the contact-mode
686 triboelectric self-powered strain sensor (Adapted from [164]).

687 The porous structure in auxetic foam provides the space for conductive components to
688 composite in, making auxetic foam itself with high electrical conductivity. Ahmed *et al.* [165] have
689 developed an AgNW (silver nanowire) - based auxetic foam sensor (**Figure. 34**). This device has
690 been trialed for air pressure detection and three-dimensional sensing. The AgNW-based auxetic
691 foam sensor possesses both improved piezoresistive sensitivity and stability in air or water. The
692 device also shows repeatable and reliable sensing performance under cyclic loading or unloading
693 situations. Other potential applications of this device as mentioned in the paper include sportswear,
694 safety gears, filtration and flow detection, smart healthcare foams and prosthetic liners.



695
696 **Figure. 34.** Schematics of (a) fabrication of the AgNW sensor and applications to (b) air pressure
697 detection and (c) three-dimensional sensing (Adapted from [165]).

698 Another interesting design of a strain-gauge sensor has been proposed on a combination of
699 multiwalled carbon nanotube/polydimethylsiloxane (MWCNT/PDMS) substrate fabricated on an
700 open-cell PU auxetic foam by Malfa *et al.* [166] (**Figure. 35**). This porous sensor could be used to
701 integrate flexible electrode and soft robotics designs.



702
703 **Figure. 35 .** Flexible carbon nanotubes-based auxetic sponge electrode for strain sensing (Adapted
704 from [166]).

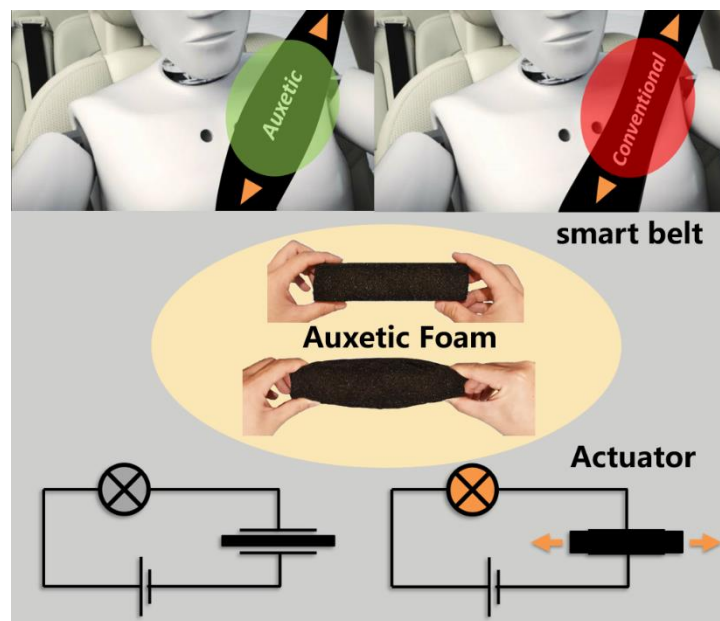
6. Challenges and perspectives

Auxetic foams could be a potential alternative to conventional foams in applications where special deformation mechanisms of the foam material play a significant role. However, most of the potential applications are limited by the substantial lack of scale-up manufacturing methodologies to produce large auxetic foam samples. The development of feasible, effective and low-cost ways to manufacture large specimens of negative Poisson's ratio foam samples is crucial to future commercialization. Methodologies of utilizing chemical reactions to soften foam ribs [50, 51] or decrease the required temperature during conversion [36, 53-55] are beneficial in eliminating heat transfer problems. Therefore, further investigation of the chemical properties of foam materials and the development of chemical conversion equipment are necessary for manufacturing scale-up of auxetic foams. Some auxetic foam specimens reported in open literature do not maintain stable mechanical properties in the long term, with samples also recovering their original shape after a period of time, or being re-subjected to heating (shape memory effect [43, 44, 121]). One could however take advantage of this feature for some specific applications (for example: if maximum volume application is an issue, one could use auxetic foams in situations where the volume available is greatly reduced, and make use of the shape memory effect to restore the porous material to its pristine side when volume available is not anymore an issue). The long-term stability of the mechanical properties is however paramount in most engineering applications (cushions and pads, for example). The further development of manufacturing procedures and methodologies to control the recovery and stability of auxetic foams would significantly improve the use of negative Poisson's ratio foams in the design at higher technology readiness levels.

A considerable number of geometric models with different deformation mechanisms [15, 30, 42, 49, 77, 79-83, 85, 87-90, 126, 134] have been proposed to simulate auxetic foams in the past decades. Those models provide explanations and predictions of specific mechanical properties to some extent. However, as a material with high heterogeneity [104] and anisotropy [126], auxetic foams cannot be accurately described by deterministic geometric modeling only. Image-based techniques like SEM and CT are able to show real and detailed micro-structure of auxetic foams [36, 39, 49, 56, 73, 85, 93, 95, 96, 98]. The more systematic use of solid models extracted from μ -CT scans and converted into FE would increase the fidelity of the modelling of auxetic foams. There are however also some issues associated to high-fidelity FE simulations of auxetic foams extracted from CT scans. The first is the need of large numbers of μ -CT volumes to be extracted from different positions of the auxetic foam block. Little is known about the effective heterogeneity distributed within a negative Poisson's ratio foam, scans tend to be expensive and take long time to be performed, most of the data available are related to a single or very few scans inside the foam blocks. The limited number of scanned volumes inside the same block of auxetic foams limits the statistical validity of the topological information that can be extracted from imaging the microstructure of the foam itself. The second issue related to the use of FE with solid models extracted from foam scans

742 is the fact that very little is known about the mechanical properties of the core polymer constituting
743 the foams. Estimates of the Young's modulus from inverse identification of the PU in auxetic PU
744 foams subjected to mechanical loading and other data from open literature vary between 10 MPa to
745 ~250 MPa [34, 167-169]. Moreover, the simulated stiffness and/or stress-strain curves from the μ -
746 CT scan FE models are heavily dependent upon the type of boundary conditions and loading applied,
747 making any direct comparison with experimental curves especially obtained from homogenized
748 auxetic foam samples quite problematic. Any technique developed to increase the number of high-
749 fidelity scans in an affordable way and improve the reliability of the FE modelling in terms of core
750 material properties and boundary conditions would significantly help the computational modelling
751 of auxetic foams. Another approach that could offer some advantages in modelling statistically
752 realistic auxetic foams is the use of 2D random models that show some similarity to the topology of
753 negative Poisson's ratio cellular materials like Thiessen polygons (Voronoi diagrams) [170-173].
754 Quite interestingly, Li *et al.* [91] have shown that by using 2D Voronoi networks to simulate Cu
755 copper foams subjected to strain hardening and biaxial compression, it is possible to predict the
756 resulting Poisson's ratio and EA capacity of the real auxetic metal foams. The use of stochastic
757 based tessellation for PU pristine foams based on Kelvin lattices or similar topologies and more in-
758 depth information about the mechanics and shape memory effect of the core PU could be
759 instrumental to create a digital twin of the manufacturing process of auxetic foams. Lakes *et al.* also
760 introduced Cosserat (micropolar) theory [174] for the analysis of materials with negative Poisson's
761 ratios [108, 175, 176], stating that syntactic foams could be regarded as classical ones apart from
762 small deviations. Rueger and Lakes however found compelling experimental evidence of the
763 existence of Cosserat torsion lengths and coupling due to size effects while testing the foams [177].
764 Gaspar *et al.* [178] developed a theoretical framework to predict the elastic properties of a material
765 with contacting microstructure originally proposed by Koenders [179] and extending the previous
766 formulation to continuum materials with auxetic behaviour and anisotropic heterogeneity.
767 Ciambella *et al.* [180] and Rueger *et al.* [181] modeled auxetic open cell foams as continuum solids
768 for the analysis of nonlinear elasticity within a modified Ogden hyperelastic anisotropic framework.
769 Recently, the group of Montáns [182, 183] provided a series of extension of phenomenological
770 linear theory, realizing the simulation of strain-stress relation and auxetic behaviour of auxetic foam
771 through an accurate numerical methodology. Such methodology makes orthotropic materials not
772 only feasible but also efficient (compared with FE analysis) simulated. However, the simulation
773 processes of their works are carried on axial quasi-static loading only, some sophisticated loading
774 conditions such as impact, crushing and cyclic loading are inescapable in applications, therefore are
775 desirable to be simulated as well. Auxetic foams produced with the current manufacturing
776 methodologies are difficult to simulate with high-fidelity continuum Cauchy classical elasticity
777 models. The theoretical approaches discussed above are an indicator for the need to further develop
778 more high-fidelity continuum theories and therefore to realistically simulate the deformation
779 mechanisms and size effects observed in real foams.

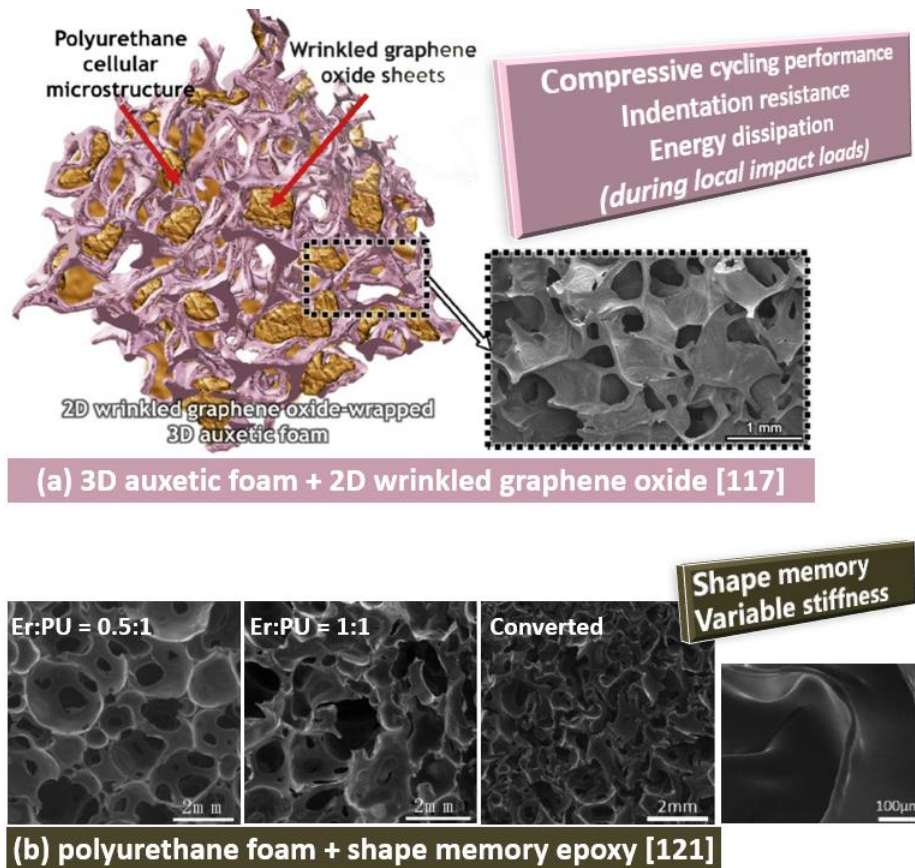
780 Another interesting and promising concept is to engineer the large lateral deformations
 781 triggered by axial loading in piezomorphic foams to design and fabricate sensors [163-166]. Soft
 782 sensors have significant potential in applications like soft robotic, biomedical and behavioral
 783 sensing, smart belts (**Figure. 36**) and smart clothing. Piezomorphic materials [34] could be also used
 784 as actuator elements by enabling turning on/off of devices in response to stress-induced shape
 785 changes (**Figure. 36**). Other potential applications are in the smart bandage sector (drugs can be
 786 released when the bandage is stretched by the swelling of the wound), adaptive airfoils (stress
 787 induced shape change), prosthetic limb lining (fit stump volume variations), bra cups (expand during
 788 vigorous exercise and/or periods of significant variations in breast size) and deployable/removable
 789 cores (easy to insert and hard to extract, a similar application of auxetic nails can be seen in ref.
 790 [184]).



791 **Figure. 36.** Examples of potential applications utilizing the unique stress-induced shape change of
 792 auxetic foam materials (middle): smart belts (upper) and actuator elements (lower).
 793

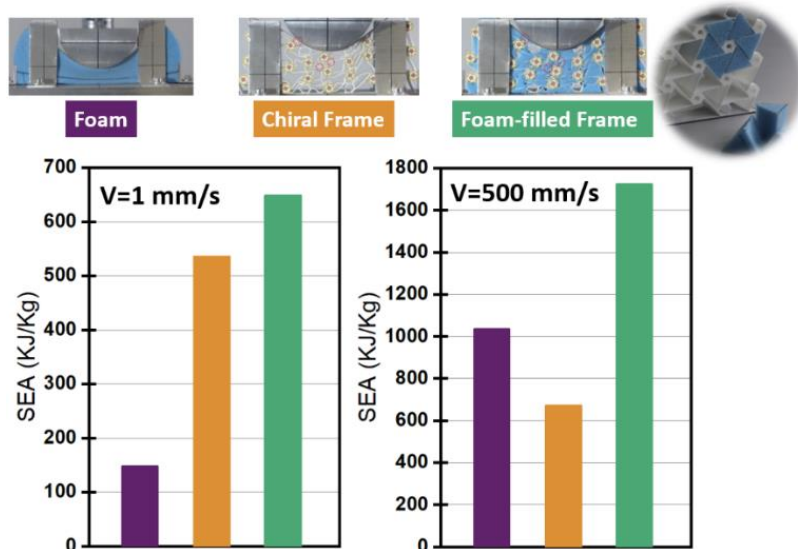
794 Composite materials and structures with auxetic foams are also promising for applications like
 795 complaint composites for prosthesis, impact and blast protection. Recently, composite structures
 796 with auxetic foams and cellular materials have been designed, modelled and built, showing
 797 interesting performances for energy [141, 152, 185] and shear resistance [19, 31, 38, 45, 83, 108,
 798 109, 111]. Compared with other traditional core materials, auxetic foams tend however to possess a
 799 low stiffness. It would be therefore interesting to develop more rigid and lightweight auxetic foams
 800 with enhanced mechanical properties, both on the polymeric and metal foam side, as well as to
 801 explore hybrid combinations of auxetic foams and other more rigid materials or structures.
 802 Lightweight characteristics are also important. Auxetic foams are denser than their pristine
 803 conventional counterpart used for the production, depending on the volumetric compression ratio.
 804 While some specific mechanical properties are significantly enhanced compared to the conventional
 805 original foam, the comparison of the specific properties (i.e., density or weight averaged) between

806 auxetic and conventional foams may not offer the same advantages as the direct ones. Besides, as a
 807 type of cellular material, auxetic foam is potential to be a candidate for matrix material, in which
 808 fluid or powder additions, such as graphene oxide [117] and Er [121], of which are easy to disperse
 809 and adhere to the foam ribs, i.e., forming composite foam materials (**Figure. 37**). Composite foams
 810 hold the superior properties provided by additional materials meanwhile retain the properties of
 811 foam materials themselves, many composite foams are still based on conventional foams [186-194],
 812 it is potential to convert those composite foams into auxetics, in that original foams could obtain
 813 triple functions.



814 **Figure. 37.** Two kinds of auxetic composite foams of (a) 2D graphene oxide-wrapped auxetic PU
 815 foam and (b) shape memory composite foam, and their functional enhancements (Adapted from [117]
 816 and [121]).

818 A series of configurations made using auxetic frames and inclusions of conventional foam
 819 have been also investigated (**Figure. 38**) [195, 196]. In a broad sense, these configurations can be
 820 defined as hybrid auxetic by increasing the bulk properties of the composite with the foam matrix
 821 and using the auxetic lattice in a synergistic way to increase the EA and impact protection.



822
823 **Figure. 38.** EA performance of foam-filled auxetic structures tested for an indentation of 50 mm
824 (Adapted from [196]).

825 In addition, rigid open-cell auxetic and metal foams could be used as scaffolds to build silicone
826 [197], mortar [156], concrete and other similar high-performance composites. Random reticular
827 structures of the foam scaffolds could contribute to oppose shear failure and fracture in these foam-
828 based composites [156].

829 Another aspect to be considered and of increasingly significant importance is the
830 environmental impact of auxetic foams, especially in view of scale-up manufacturing processes. All
831 the manufacturing processes used to fabricate polymeric foams, in particular, necessity of either
832 temperature and/or use of chemicals. Considering the contribution of tooling, molding and labor,
833 detailed life cycle costs of the different manufacturing processes are needed to make the business
834 and environmental case for the large-scale manufacturing of auxetic foams. The use of more bio-
835 based polymers and products during the manufacturing is also an interesting aspect to be considered.

836 7. Conclusions

837 In this paper, the state-of-the-art of manufacturing, characteristics and applications of auxetic
838 foams have been reviewed. Existing methodologies for the conversion of auxetic foams have been
839 presented and focus has been put on the relations between the different possible manufacturing
840 parameters and recommended optimal combinations of those. The micro-structure and deformation
841 mechanisms in auxetic foams have been discussed, from theoretical unit cell models to more high-
842 fidelity numerical ones based on geometry information extracted from imaging techniques. The
843 mechanical properties of auxetic foams have been considered here in terms of stiffness, hardness
844 and toughness, showing superior performance in loadings like indentation, impact, cyclic and
845 vibroacoustic. Auxetic foams could represent enhanced alternatives to conventional foams in many
846 applications where unusual deformation mechanisms of the foam material play a role. We have also
847 provided a consistent number of examples of novel applications of auxetic ranging from biomedical,
848 aerospace, filtration and sensing, to name a few. This paper also provides a discussion of existing

849 challenges and future research directions to enhance the feasibility and the design space of auxetic
850 foam materials and structures.

851 **Acknowledgments**

852 This work was supported by the National Natural Science Foundation of China (grant numbers
853 51978330, 51778283); National Natural Science Foundation for the Youth of China (grant number
854 51808286); Natural Science Foundation of Jiangsu Province (grant number BK20180710); and the
855 Innovation Project for Graduate Student of Jiangsu Province (grant number KYCX20_1009). FS
856 would like to acknowledge the support of the UK Engineering and Physical Sciences Research
857 Council (EPSRC) EP/R032793/1 SYSDYMATS project. FS is also grateful to Dr Qicheng Zhang
858 from the Bristol Composites Institute for the discussions about the FE modelling.

859 **References:**

- 860 [1] Fung YC. Foundations of Solid Mechanics. Prentice-Hall 1965:525.
861 [2] Voigt W. Allgemeine formeln für die bestimmung der elasticitätsconstanten von krystallen durch die
862 beobachtung der biegun und drillung von prismen. Ann Phys 1882;252:398-416.
863 [3] Evans KE. Auxetic polymers: a new range of materials. Endeavour 1991;15:170-4.
864 [4] Love A. A treatise on the mathematical theory of elasticity 1892.
865 [5] Lees C, Vincent JFV, Hillerton JE. Poisson's ratio in skin. Biomed Mater Eng 1991;1:19-23.
866 [6] Veronda DR, Westmann RA. Mechanical characterization of skin-finite deformations. J Biomech
867 1970;3:111-24.
868 [7] Williams JL, Lewis JL. Properties and an anisotropic model of cancellous bone from the proximal tibial
869 epiphysis. J Biomech Eng 1982;104:50-6.
870 [8] Baughman RH. Auxetic materials: avoiding the shrink. Nature 2003;425:667.
871 [9] Wojciechowski KW. Constant thermodynamic tension Monte Carlo studies of elastic properties of a
872 two-dimensional system of hard cyclic hexamers. Mol Phys 1987;61:1247-58.
873 [10] Hou J, Zhao G, Zhang L, Wang G, Li B. High-expansion polypropylene foam prepared in non-
874 crystalline state and oil adsorption performance of open-cell foam. J Colloid Interface Sci
875 2019;542:233-42.
876 [11] Wang G, Zhao G, Dong G, Mu Y, Park CB, Wang G. Lightweight, super-elastic, and thermal-sound
877 insulation bio-based PEBA foams fabricated by high-pressure foam injection molding with mold-
878 opening. Eur Polym J 2018;103:68-79.
879 [12] Tiuc AE, Nemeş O, Vermeşan H, Toma AC. New sound absorbent composite materials based on sawdust
880 and polyurethane foam. Compos B Eng 2019;165:120-30.
881 [13] Rizvi A, Chu RK, Lee JH, Park CB. Superhydrophobic and oleophilic open-cell foams from fibrillar
882 blends of polypropylene and polytetrafluoroethylene. ACS Appl Mater Interfaces 2014;6:21131-40.
883 [14] Zhou J, Guan ZW, Cantwell WJ. The impact response of graded foam sandwich structures. Compos
884 Struct 2013;97:370-7.
885 [15] Lakes R. Foam structures with a negative Poisson's ratio. Science 1987;235:1038-40.
886 [16] Greaves GN, Greer AL, Lakes RS, Rouxel T. Poisson's ratio and modern materials. Nat Mater
887 2011;10:823-37.
888 [17] Ren X, Shen J, Tran P, Ngo TD, Xie YM. Design and characterisation of a tuneable 3D buckling-induced
889 auxetic metamaterial. Mater Des 2018;139:336-42.
890 [18] Ren X, Shen J, Ghaedizadeh A, Tian H, Min Xie Y. Experiments and parametric studies on 3D metallic
891 auxetic metamaterials with tuneable mechanical properties. Smart Mater Struct 2015;24:095016.
892 [19] Evans KE, Alderson A. Auxetic materials: Functional materials and structures from lateral thinking!
893 Adv Mater 2000;12:617.
894 [20] Zhai X, Gao J, Liao H, Kirk CD, Balogun YA, Chen WW. Mechanical behaviors of auxetic polyurethane
895 foam at quasi-static, intermediate and high strain rates. Int J Impact Eng 2019;129:112-8.
896 [21] Novak N, Vesenjak M, Ren Z. Auxetic cellular materials - A review. Mech Eng 2016;62:485-93.
897 [22] Susmita Naik RDD, C. N. Wani, and S. K. Giri. A review on various aspects of auxetic materials. AIP
898 Conf Proc 2015:020004.
899 [23] Duncan O, Shepherd T, Moroney C, Foster L, Venkatraman P, Winwood K, et al. Review of auxetic

-
- 900 materials for sports applications: expanding options in comfort and protection. *Appl Sci* 2018;8:941.
- 901 [24] Kelkar PU, Kim HS, Cho KH, Kwak JY, Kang CY, Song HC. Cellular auxetic structures for mechanical
902 metamaterials: A review. *Sensors (Basel)* 2020;20:3132.
- 903 [25] Saxena KK, Das R, Calius EP. Three decades of auxetics research - materials with negative Poisson's
904 ratio: A review. *Adv Eng Mater* 2016;18:1847-70.
- 905 [26] Ren X, Das R, Tran P, Ngo TD, Xie YM. Auxetic metamaterials and structures: A review. *Smart Mater*
906 *Struct* 2018;27:023001.
- 907 [27] Luo C, Han CZ, Zhang XY, Zhang XG, Ren X, Xie YM. Design, manufacturing and applications of
908 auxetic tubular structures: A review. *Thin-Walled Struct* 2021;163:107682.
- 909 [28] Zhang J, Lu G, You Z. Large deformation and energy absorption of additively manufactured auxetic
910 materials and structures: A review. *Compos B Eng* 2020;201.
- 911 [29] Critchley R, Corni I, Wharton JA, Walsh FC, Wood RJK, Stokes KR. A review of the manufacture,
912 mechanical properties and potential applications of auxetic foams. *Phys Status Solidi B*
913 2013;250:1963-82.
- 914 [30] Friis EA, Lakes RS, Park JB. Negative Poisson's ratio polymeric and metallic foams. *J Mater Sci*
915 1988;23:4406-14.
- 916 [31] Choi JB, Lakes RS. Fracture toughness of re-entrant foam materials with a negative Poisson's ratio:
917 experiment and analysis. *Int J Fract* 1996;80:73-83.
- 918 [32] Chen CP, Lakes RS. Holographic study of conventional and negative Poisson's ratio metallic foams:
919 elasticity, yield and micro-deformation. *J Mater Sci* 1991;26:5397-402.
- 920 [33] Li D, Dong L, Lakes RS. The properties of copper foams with negative Poisson's ratio via resonant
921 ultrasound spectroscopy. *Phys Status Solidi B* 2013;250:1983-7.
- 922 [34] Alderson K, Alderson A, Ravirala N, Simkins V, Davies P. Manufacture and characterisation of thin flat
923 and curved auxetic foam sheets. *Phys Status Solidi B* 2012;249:1315-21.
- 924 [35] Allen T, Hewage T, Newton-Mann C, Wang W, Duncan O, Alderson A. Fabrication of auxetic foam
925 sheets for sports applications. *Phys Status Solidi B* 2017;254:1700596.
- 926 [36] Fan D, Li M, Qiu J, Xing H, Jiang Z, Tang T. Novel method for preparing auxetic foam from closed-
927 cell polymer foam based on the steam penetration and condensation process. *ACS Appl Mater*
928 *Interfaces* 2018;10:22669-77.
- 929 [37] Chiang Fp. Manufacturing and characterization of an auxetic composite. In: TMS, editor. Supplemental
930 Proceedings: Materials Processing and Interfaces 2012.
- 931 [38] Chan N, Evans KE. Fabrication methods for auxetic foams. *J Mater Sci* 1997;32:5945-53.
- 932 [39] Mohsenizadeh S, Ahmad Z, Alipour R, Majid RA, Prawoto Y. Quasi tri-axial method for the fabrication
933 of optimized polyurethane auxetic foams. *Phys Status Solidi B* 2019;256:1800587.
- 934 [40] Duncan O, Foster L, Senior T, Allen T, Alderson A. A comparison of novel and conventional fabrication
935 methods for auxetic foams for sports safety applications. *Procedia Eng* 2016;147:384-9.
- 936 [41] Sanami M, Alderson A, Alderson KL, McDonald SA, Mottershead B, Withers PJ. The production and
937 characterization of topologically and mechanically gradient open-cell thermoplastic foams. *Smart*
938 *Mater Struct* 2014;23:055016.
- 939 [42] Duncan O, Allen T, Foster L, Senior T, Alderson A. Fabrication, characterisation and modelling of
940 uniform and gradient auxetic foam sheets. *Acta Mater* 2017;126:426-37.
- 941 [43] Bianchi M, Scarpa F, Smith CW. Shape memory behaviour in auxetic foams: Mechanical properties.
942 *Acta Mater* 2010;58:858-65.
- 943 [44] Bianchi M, Scarpa F, Smith CW, Whittell GR. Physical and thermal effects on the shape memory
944 behaviour of auxetic open cell foams. *J Mater Sci* 2010;45:341-7.
- 945 [45] Martz EO, Lee, T., Lakes, R. S., Goel, V. K., & Park, J. B. . Re-entrant transformation methods in closed
946 cell foams. *Cell Polym* 1996;15:229-49.
- 947 [46] Bianchi M, Scarpa F, Banse M, Smith CW. Novel generation of auxetic open cell foams for curved and
948 arbitrary shapes. *Acta Mater* 2011;59:686-91.
- 949 [47] Zhang Q, Lu W, Scarpa F, Barton D, Lakes RS, Zhu Y, et al. Large stiffness thermoformed open cell
950 foams with auxeticity. *Appl Mater Today* 2020;20:100775.
- 951 [48] Najarian F, Alipour R, Shokri Rad M, Nejad AF, Razavykia A. Multi-objective optimization of
952 converting process of auxetic foam using three different statistical methods. *Measurement*
953 2018;119:108-16.
- 954 [49] Smith CW, Grima JN, Evans KE. A novel mechanism for generating auxetic behaviour in reticulated
955 foams: Missing rib foam model. *Acta Mater* 2000;48:4349-56.
- 956 [50] Grima JN, Attard D, Gatt R, Cassar RN. A novel process for the manufacture of auxetic foams and for
957 their re-conversion to conventional form. *Adv Eng Mater* 2009;11:533-5.
- 958 [51] Lisiecki J, Błażejczak T, Kłysz S, Gmurczyk G, Reymer P, Mikułowski G. Tests of polyurethane foams

959 with negative Poisson's ratio. *Phys Status Solidi B* 2013;250:1988-95.

960 [52] Lisiecki J, Nowakowski D. The Impact of Technology on Poisson's Ratio of Auxetic Polyurethane
961 Foams. *Aviat Adv Maint* 2018;41:119-60.

962 [53] Li Y, Zeng C. Room-temperature, near-instantaneous fabrication of auxetic materials with constant
963 poisson's ratio over large deformation. *Adv Mater* 2016;28:2822-6.

964 [54] Fan D, Shi Z, Li N, Qiu J, Xing H, Jiang Z, et al. Novel method for preparing a high-performance
965 auxetic foam directly from polymer resin by a one-pot CO₂ foaming process. *ACS Appl Mater*
966 *Interfaces* 2020;12:48040-8.

967 [55] Duncan O, Allen T, Birch A, Foster L, Hart J, Alderson A. Effect of steam conversion on the cellular
968 structure, Young's modulus and negative Poisson's ratio of closed-cell foam. *Smart Mater Struct*
969 2021;30:015031.

970 [56] Critchley R, Corni I, Wharton JA, Walsh FC, Wood RJK, Stokes KR. The preparation of auxetic foams
971 by three-dimensional printing and their characteristics. *Adv Eng Mater* 2013:980-5.

972 [57] Jayavardhan ML, Doddamani M. Quasi-static compressive response of compression molded glass
973 microballoon/HDPE syntactic foam. *Compos B Eng* 2018;149:165-77.

974 [58] Osman MM, Shazly M, El-Danaf EA, Jamshidi P, Attallah MM. Compressive behavior of stretched and
975 composite microlattice metamaterial for energy absorption applications. *Compos B Eng* 2020;184.

976 [59] Curd ME, Morrison NF, Smith MJA, Gajjar P, Yousaf Z, Parnell WJ. Geometrical and mechanical
977 characterisation of hollow thermoplastic microspheres for syntactic foam applications. *Compos B Eng*
978 2021;223.

979 [60] D'Auria M, Davino D, Pantani R, Sorrentino L. Magnetic field-structuring as versatile approach to shape
980 the anisotropic mechanical response of composite foams. *Compos B Eng* 2021;212.

981 [61] Singh AK, Shishkin A, Koppel T, Gupta N. A review of porous lightweight composite materials for
982 electromagnetic interference shielding. *Compos B Eng* 2018;149:188-97.

983 [62] Jiang H, Coomes A, Zhang Z, Ziegler H, Chen Y. Tailoring 3D printed graded architected polymer
984 foams for enhanced energy absorption. *Compos B Eng* 2021;224.

985 [63] Song J, Wang Y, Zhou W, Fan R, Yu B, Lu Y, et al. Topology optimization-guided lattice composites
986 and their mechanical characterizations. *Compos B Eng* 2019;160:402-11.

987 [64] Meng J, Liu T-W, Wang H-Y, Dai L-H. Ultra-high energy absorption high-entropy alloy syntactic foam.
988 *Compos B Eng* 2021;207.

989 [65] Wang Q, Li Z, Zhang Y, Cui S, Yang Z, Lu Z. Ultra-low density architected metamaterial with superior
990 mechanical properties and energy absorption capability. *Compos B Eng* 2020;202.

991 [66] Wang Y, Lakes R, Butenhoff A. Influence of cell size on re-entrant transformation of negative Poisson's
992 ratio reticulated polyurethane foams. *Cell Polym* 2001;20:373-85.

993 [67] Choi JB, Lakes RS. Non-linear properties of polymer cellular materials with a negative Poisson's ratio.
994 *J Mater Sci* 1992;27:4678-84.

995 [68] Duncan O, Clegg F, Essa A, Bell AMT, Foster L, Allen T, et al. Effects of heat exposure and volumetric
996 compression on Poisson's ratios, Young's moduli, and polymeric composition during thermo-
997 mechanical conversion of auxetic open cell polyurethane foam. *Phys Status Solidi B*
998 2019;256:1800393.

999 [69] Bianchi M, Scarpa FL, Smith CW. Stiffness and energy dissipation in polyurethane auxetic foams. *J*
1000 *Mater Sci* 2008;43:5851-60.

1001 [70] Critchley R, Smy V, Corni I, Wharton JA, Walsh FC, Wood RJK, et al. Experimental and computation
1002 assessment of thermomechanical effects during auxetic foam fabrication. *Sci Rep* 2020;10:18301.

1003 [71] Lowe A, Lakes RS. Negative Poisson's ratio foam as seat cushion material. *Cell Polym.* 2000;19:157-
1004 67.

1005 [72] Duncan O, Allen T, Foster L, Gatt R, Grima JN, Alderson A. Controlling density and modulus in auxetic
1006 foam fabrications - implications for impact and indentation testing. *Proceedings* 2018;2:250.

1007 [73] Chaithanya Vinay V, Mohan Varma DS. Fabrication and testing of auxetic foams for rehabilitation
1008 applications. *J Indian Inst Sci* 2019;99:511-8.

1009 [74] Khaderi SN, Kumar N, Rao KT. Impact on auxetic and metal foams. *Vibroeng Proc* 2019;29:255-9.

1010 [75] Wei G. Negative and conventional Poisson's ratios of polymeric networks with special microstructures.
1011 *J Chem Phys* 1992;96:3226-33.

1012 [76] Warren WE, Kraynik AM. Foam mechanics - the Linear elastic response of two-dimensional spatially
1013 periodic cellular materials. *Mech Mater* 1987;6:27-37.

1014 [77] Choi JB, Lakes RS. Nonlinear analysis of the Poisson's ratio of negative Poisson's ratio foams. *J Compos*
1015 *Mater* 2016;29:113-28.

1016 [78] Doyoyo M, Wanhu J. Plastic failure analysis of an auxetic foam or inverted strut lattice under
1017 longitudinal and shear loads. *J Mech Phys Solids* 2006;54:1479-92.

-
- 1018 [79] Chan N, Evans KE. Microscopic examination of the microstructure and deformation of conventional
1019 and auxetic foams. *J Mater Sci* 1997;32:5725-36.
- 1020 [80] Scarpa F, Yates JR, Ciffo LG, Patsias S. Dynamic crushing of auxetic open-cell polyurethane foam.
1021 *Proc Inst Mech Eng Part C-J Eng Mech Eng Sci* 2002;216:1153-6.
- 1022 [81] Alderson A. A triumph of lateral thought. *Chem Ind* 1999:384-91.
- 1023 [82] Alderson A, Rasburn J, Evans KE, Grima JN. Auxetic polymeric filters display enhanced de-fouling
1024 and pressure compensation properties. *J Membr Sci Technol* 2001;2001:6-8.
- 1025 [83] Chan N, Evans KE. The mechanical properties of conventional and auxetic foams. Part II: Shear. *J Cell*
1026 *Plast* 2016;35:166-83.
- 1027 [84] Gaspar N, Ren X, Smith C, Grima J, Evans K. Novel honeycombs with auxetic behaviour. *Acta Mater*
1028 2005;53:2439-45.
- 1029 [85] Lim TC, Alderson A, Alderson KL. Experimental studies on the impact properties of auxetic materials.
1030 *Phys Status Solidi B* 2014;251:307-13.
- 1031 [86] Gaspar N, Smith CW, Miller EA, Seidler GT, Evans KE. Quantitative analysis of the microscale of
1032 auxetic foams. *Phys Status Solidi B* 2005;242:550-60.
- 1033 [87] Grima JN, Evans KE. Auxetic behavior from rotating triangles. *J Mater Sci* 2006;41:3193-6.
- 1034 [88] Grima JN, Chetcuti E, Manicaro E, Attard D, Camilleri M, Gatt R, et al. On the auxetic properties of
1035 generic rotating rigid triangles. *Proc R Soc A-Math Phys Eng Sci* 2011;468:810-30.
- 1036 [89] Chetcuti E, Ellul B, Manicaro E, Brincat J-P, Attard D, Gatt R, et al. Modeling auxetic foams through
1037 semi-rigid rotating triangles. *Phys Status Solidi B* 2014;251:297-306.
- 1038 [90] Pozniak AA, Smardzewski J, Wojciechowski KW. Computer simulations of auxetic foams in two
1039 dimensions. *Smart Mater Struct* 2013;22:084009.
- 1040 [91] Li D, Dong L, Yin JH, Lakes RS. Negative Poisson's ratio in 2D Voronoi cellular solids by biaxial
1041 compression: a numerical study. *J Mater Sci* 2016;51:7029-37.
- 1042 [92] Alderson A, Alderson KL, Davies P, Smart G. The effects of processing on the topology and mechanical
1043 properties of negative Poisson's ratio foams. *Int Mech Eng Congress Expo* 2005.
- 1044 [93] McDonald SA, Dedreuil-Monet G, Yao YT, Alderson A, Withers PJ. In situ 3D X-ray microtomography
1045 study comparing auxetic and non-auxetic polymeric foams under tension. *Phys Status Solidi B*
1046 2011;248:45-51.
- 1047 [94] McDonald SA, Ravirala N, Withers PJ, Alderson A. In situ three-dimensional X-ray microtomography
1048 of an auxetic foam under tension. *Scr Mater* 2009;60:232-5.
- 1049 [95] Elliott JA, Windle AH, Hobdell JR, Eeckhaut G, Oldman RJ, Ludwig W, et al. In-situ deformation of
1050 an open-cell flexible polyurethane foam characterised by 3D computed microtomography. *J Mater Sci*
1051 2002;37:1547-55.
- 1052 [96] Li Y, Zeng C. On the successful fabrication of auxetic polyurethane foams: Materials requirement,
1053 processing strategy and conversion mechanism. *Polymer* 2016;87:98-107.
- 1054 [97] Pierron F, McDonald SA, Hollis D, Fu J, Withers PJ, Alderson A. Comparison of the mechanical
1055 behaviour of standard and auxetic foams by X-ray computed tomography and digital volume
1056 correlation. *Strain* 2013;49:467-82.
- 1057 [98] Pierron F. Identification of Poisson's ratios of standard and auxetic low-density polymeric foams from
1058 full-field measurements. *J Strain Anal Eng Des* 2010;45:233-53.
- 1059 [99] Lisiecki J, Kłysz S, Błażejewicz T, Gmurczyk G, Reymer P. Tomographic examination of auxetic
1060 polyurethane foam structures. *Phys Status Solidi B* 2014;251:314-20.
- 1061 [100] Pashine N, Hexner D, Liu AJ, Nagel SR. Directed aging, memory, and nature's greed. *Sci Adv*
1062 2019;5:eaax4215.
- 1063 [101] Lv W, Li D, Dong L. Study on blast resistance of a composite sandwich panel with isotropic foam core
1064 with negative Poisson's ratio. *Int J Mech Sci* 2021;191.
- 1065 [102] Mikulich Olena SL, Povstiana Yulia. Dynamic stress state of auxetic foam medium under the action
1066 of impulse load. *Advances in Design, Simulation and Manufacturing II* 2020. p. 623-32.
- 1067 [103] Mott PH, Roland CM. Limits to Poisson's ratio in isotropic materials. *Phys Rev B* 2009;80:132104.
- 1068 [104] Gaspar N. Estimates for the localised stiffness and heterogeneity of auxetic foams. *Phys Status Solidi*
1069 *B* 2008;245:497-501.
- 1070 [105] Mott PH, Roland CM. Limits to Poisson's ratio in isotropic materials - general result for arbitrary
1071 deformation. *Phys Scr* 2013;87:055404.
- 1072 [106] Roh JH, Giller CB, Mott PH, Roland CM. Failure of classical elasticity in auxetic foams. *AIP Adv*
1073 2013;3:042126.
- 1074 [107] Roland CM, Mott PH, Calvo DC, Walker CN, Guild MD. Deviation from classical elasticity in the
1075 acoustic response of auxetic foams. *Rubber Chem Technol* 2017;90:381-6.
- 1076 [108] Lakes RS. Design considerations for materials with negative Poisson's ratios. *J Mater Sci*

- 1077 1993;115:696-700.
- 1078 [109] Choi J, Lakes R. Design of a fastener based on negative Poisson's ratio foam. *Cell Polym* 1991;10:205-
1079 12.
- 1080 [110] Novak N, Duncan O, Allen T, Alderson A, Vesenjak M, Ren Z. Shear modulus of conventional and
1081 auxetic open-cell foam. *Mech Mater.* 2021;157:103818.
- 1082 [111] Cheng HC, Scarpa F, Panzera TH, Farrow I, Peng H-X. Shear stiffness and energy absorption of auxetic
1083 open cell foams as sandwich cores. *Phys Status Solidi B* 2019;256:1800411
- 1084 [112] Bianchi M, Scarpa F. Vibration transmissibility and damping behaviour for auxetic and conventional
1085 foams under linear and nonlinear regimes. *Smart Mater Struct* 2013;22:084010.
- 1086 [113] Scarpa F, Ciffo LG, Yates JR. Dynamic properties of high structural integrity auxetic open cell foam.
1087 *Smart Mater Struct* 2004;13:49-56.
- 1088 [114] Scarpa F, Bullough WA, Lumley P. Trends in acoustic properties of iron particle seeded auxetic
1089 polyurethane foam. *Proc Inst Mech Eng Part C-J Eng Mech Eng Sci* 2005;218:241-4.
- 1090 [115] Scarpa F, Smith FC. Passive and MR fluid-coated auxetic PU foam - mechanical, acoustic, and
1091 electromagnetic properties. *J Intell Mater Syst Struct* 2016;15:973-9.
- 1092 [116] Chekkal I, Bianchi M, Remillat C, Bécot FX, Jaouen L, Scarpa F. Vibro-acoustic properties of auxetic
1093 open cell foam: Model and experimental results. *Acta Acust United Acust* 2010;96:266-74.
- 1094 [117] Hwan OJ, Seok KJ, Hiep NV, Kwon OI. Auxetic graphene oxide-porous foam for acoustic wave and
1095 shock energy dissipation. *Compos B Eng* 2020;186:107817.
- 1096 [118] Gravade M OM, Collet M, Scarpa F, Bianchi M, Ichchou M. Auxetic transverse isotropic foams: from
1097 experimental efficiency to model correlation. *Proceedings of the Acoustics. Nantes* 2012.
- 1098 [119] Alderson A, Rasburn J, Evans KE. Mass transport properties of auxetic (negative Poisson's ratio) foams.
1099 *Phys Status Solidi B* 2007;244:817-27.
- 1100 [120] Gatt R, Attard D, Manicaro E, Chetcuti E, Grima JN. On the effect of heat and solvent exposure on the
1101 microstructure properties of auxetic foams: A preliminary study. *Phys Status Solidi B.* 2011;248:39-44.
- 1102 [121] Yao Y, Luo Y, Xu Y, Wang B, Li J, Deng H, et al. Fabrication and characterization of auxetic shape
1103 memory composite foams. *Compos B Eng* 2018;152:1-7.
- 1104 [122] N. Chan KEE. Indentation resilience of conventional and auxetic foams. *J Cell Plast* 1998;34:231-60.
- 1105 [123] Bhullar SK. Characterization of auxetic polyurethanes foam for biomedical implants. *e-Polymers*
1106 2014;14:441-7.
- 1107 [124] Li D, Gao R, Dong L, Lam W-K, Zhang F. A novel 3D re-entrant unit cell structure with negative
1108 Poisson's ratio and tunable stiffness. *Smart Mater Struct* 2020;29.
- 1109 [125] Pastorino P, Scarpa F, Patsias S, Yates JR, Haake SJ, Ruzzene M. Strain rate dependence of stiffness
1110 and Poisson's ratio of auxetic open cell PU foams. *Phys Status Solidi B* 2007;244:955-65.
- 1111 [126] Dirrenberger J, Forest S, Jeulin D. Effective elastic properties of auxetic microstructures: anisotropy
1112 and structural applications. *Int J Mech Mater Des* 2012;9:21-33.
- 1113 [127] Grima JN, Ravirala N, Galea R, Ellul B, Attard D, Gatt R, et al. Modelling and testing of a foldable
1114 macrostructure exhibiting auxetic behaviour. *Phys Status Solidi B* 2011;248:117-22.
- 1115 [128] Yang S, Qi C, Wang D, Gao R, Hu H, Shu J. A comparative study of ballistic resistance of sandwich
1116 panels with aluminum foam and auxetic honeycomb cores. *Adv Mech Eng* 2015;5:589216.
- 1117 [129] Scarpa F, Pastorino P, Garelli A, Patsias S, Ruzzene M. Auxetic compliant flexible PU foams: static
1118 and dynamic properties. *Phys Status Solidi B* 2005;242:681-94.
- 1119 [130] Lakes RS, Elms K. Indentability of conventional and negative Poisson's ratio foams. *J Compos Mater*
1120 2016;27:1193-202.
- 1121 [131] Bezazi A, Scarpa F. Tensile fatigue of conventional and negative Poisson's ratio open cell PU foams.
1122 *Int J Fatigue* 2009;31:488-94.
- 1123 [132] Sanami M, Ravirala N, Alderson K, Alderson A. Auxetic materials for sports applications. *Procedia*
1124 *Eng* 2014;72:453-8.
- 1125 [133] Kumar N, Khaderi SN, Tirumala Rao K. Elasto-plastic indentation of auxetic and metal foams. *J Appl*
1126 *Mech* 2020;87:011006.
- 1127 [134] Więcek T, Wasilewski A. Stiffness of auxetic foams. *Acta Phys Pol A* 2017;132:182-4.
- 1128 [135] Li D, Dong L, Lakes RS. A unit cell structure with tunable Poisson's ratio from positive to negative.
1129 *Mater Lett* 2016;164:456-9.
- 1130 [136] Wang YC, Lakes R. Analytical parametric analysis of the contact problem of human buttocks and
1131 negative Poisson's ratio foam cushions. *Int J Solids Struct* 2002;39:4825-38.
- 1132 [137] Allen T, Shepherd J, Hewage TAM, Senior T, Foster L, Alderson A. Low-kinetic energy impact
1133 response of auxetic and conventional open-cell polyurethane foams. *Phys Status Solidi B*
1134 2015;252:1631-9.
- 1135 [138] Duncan O, Foster L, Senior T, Alderson A, Allen T. Quasi-static characterisation and impact testing of

1136 auxetic foam for sports safety applications. *Smart Mater Struct* 2016;25:054014.

1137 [139] Mohsenizadeh S, Alipour R, Shokri Rad M, Farokhi Nejad A, Ahmad Z. Crashworthiness assessment
1138 of auxetic foam-filled tube under quasi-static axial loading. *Mater Des* 2015;88:258-68.

1139 [140] Mohsenizadeh S, Ahmad Z. Auxeticity effect on crushing characteristics of auxetic foam-filled square
1140 tubes under axial loading. *Thin-Walled Struct* 2019;145:106379.

1141 [141] Mohsenizadeh S, Ahmad Z, Alias A. Numerical prediction on the crashworthiness of circular and
1142 square thin-walled tubes with polymeric auxetic foam core. *J Mater Eng Perform* 2020;29:3092-106.

1143 [142] Yin H, Wen G, Liu Z, Qing Q. Crashworthiness optimization design for foam-filled multi-cell thin-
1144 walled structures. *Thin-Walled Struct* 2014;75:8-17.

1145 [143] Zarei HR, Kröger M. Crashworthiness optimization of empty and filled aluminum crash boxes. *Int J*
1146 *Crashworthiness* 2007;12:255-64.

1147 [144] F. Scarpa JG, Y. Zhang, P. Pastorino. Mechanical performance of auxetic polyurethane foam for
1148 antivibration glove applications. *Cell Polym* 2005;24: 253-68.

1149 [145] Allen T, Duncan O, Foster L, Senior T, Zampieri D, Edeh V, et al. Auxetic foam for snow-sport safety
1150 devices. *Snow Sports Trauma and Safety* 2017. p. 145-59.

1151 [146] Hou S, Liu T, Zhang Z, Han X, Li Q. How does negative Poisson's ratio of foam filler affect
1152 crashworthiness? *Mater Des* 2015;82:247-59.

1153 [147] Li D, Yin J, Dong L, Lakes RS. Strong re-entrant cellular structures with negative Poisson's ratio. *J*
1154 *Mater Sci* 2017;53:3493-9.

1155 [148] Lv W, Li D, Dong L. Study on mechanical properties of a hierarchical octet-truss structure. *Compos*
1156 *Struct* 2020;249.

1157 [149] Bezazi A, Scarpa F. Mechanical behaviour of conventional and negative Poisson's ratio thermoplastic
1158 polyurethane foams under compressive cyclic loading. *Int J Fatigue* 2007;29:922-30.

1159 [150] Mohanraj H, Filho Ribeiro SLM, Panzera TH, Scarpa F, Farrow IR, Jones R, et al. Hybrid auxetic
1160 foam and perforated plate composites for human body support. *Phys Status Solidi B* 2016;253:1378-
1161 86.

1162 [151] Foster L, Peketi P, Allen T, Senior T, Duncan O, Alderson A. Application of auxetic foam in sports
1163 helmets. *Appl Sci* 2018;8:354.

1164 [152] Mohsenizadeh S, Alipour R, Nejad AF, Rad MS, Ahmad Z. Experimental investigation on energy
1165 absorption of auxetic foam-filled thin-walled square tubes under quasi-static loading. *Procedia Manuf*
1166 2015;2:331-6.

1167 [153] Zhang XY, Wang XY, Ren X, Xie YM, Wu Y, Zhou YY, et al. A novel type of tubular structure with
1168 auxeticity both in radial direction and wall thickness. *Thin-Walled Struct* 2021;163:107758.

1169 [154] Zhanga XY, Ren X, Wang XY, Zhang Y, Xie YM. A novel combined auxetic tubular structure with
1170 enhanced tunable stiffness. *Compos B Eng* 2021.

1171 [155] Strek T, Michalski J, Jopek H. Computational analysis of the mechanical impedance of the sandwich
1172 beam with auxetic metal foam core. *Phys Status Solidi B* 2019;256:1800423.

1173 [156] Zahra T, Dhanasekar M. Characterisation of cementitious polymer mortar - Auxetic foam composites.
1174 *Constr Build Mater* 2017;147:143-59.

1175 [157] Huang TT, Ren X, Zeng Y, Zhang Y, Luo C, Zhang XY, et al. Based on auxetic foam: A novel type of
1176 seismic metamaterial for Lamb waves. *Eng Struct* 2021;246.

1177 [158] Lim TC. Torsion of semi-auxetic rods. *J Mater Sci* 2011;46:6904-9.

1178 [159] Lim TC. Auxeticity of concentric auxetic-conventional foam rods with high modulus interface
1179 adhesive. *Materials (Basel)* 2018;11:223.

1180 [160] Alderson A, Rasburn J, Ameer-Beg S, Mullarkey PG, Perrie W, Evans KE. An auxetic filter: A
1181 tuneable filter displaying enhanced size selectivity or defouling properties. *Ind Eng Chem Res*
1182 2000;39:654-65.

1183 [161] Bullogh WA, Scarpa F. Electrically controlled extension effects in soft solids. *Int J Mod Phys B*
1184 2005;19:1655-60.

1185 [162] Scarpa F, Bullough WA, Ruzzene M. Acoustic properties of auxetic foams with MR fluids. *Noise*
1186 *Control and Acoustics* 2003. p. 189-96.

1187 [163] Alderson A, Alderson KL, McDonald SA, Mottershead B, Nazare S, Withers PJ, et al. Piezomorphic
1188 materials. *Macromol Mater Eng* 2013;298:318-27.

1189 [164] Zhang SL, Lai Y-C, He X, Liu R, Zi Y, Wang ZL. Auxetic foam-based contact-mode triboelectric
1190 nanogenerator with highly sensitive self-powered strain sensing capabilities to monitor human body
1191 movement. *Adv Funct Mater* 2017;27:1606695.

1192 [165] Ahmed MF, Li Y, Zeng C. Stretchable and compressible piezoresistive sensors from auxetic foam and
1193 silver nanowire. *Mater Chem Phys* 2019;229:167-73.

1194 [166] La Malfa F, Puce S, Rizzi F, De Vittorio M. A flexible carbon nanotubes-based auxetic sponge electrode

-
- 1195 for strain sensors. *Nanomaterials* (Basel) 2020;10:2365.
- 1196 [167] Qi HJ, Boyce MC. Stress–strain behavior of thermoplastic polyurethanes. *Mech Mater* 2005;37:817-1197 39.
- 1198 [168] Somarathna HMCC, Raman SN, Mohotti D, Mutalib AA, Badri KH. Hyper-viscoelastic constitutive models for predicting the material behavior of polyurethane under varying strain rates and uniaxial tensile loading. *Constr Build Mater* 2020;236:117417.
- 1201 [169] Lu W, Qin F, Wang Y, Luo Y, Wang H, Scarpa F, et al. Engineering graphene wrinkles for large enhancement of interlaminar friction enabled damping capability. *ACS Appl Mater Interfaces* 2019;11:30278-89.
- 1204 [170] Jacobs LJM, Danen KCH, Kemmere MF, Keurentjes JTF. Quantitative morphology analysis of polymers foamed with supercritical carbon dioxide using Voronoi diagrams. *Comput Mater Sci* 2007;38:751-8.
- 1207 [171] Bouakba M, Bezazi A, Scarpa F. FE analysis of the in-plane mechanical properties of a novel Voronoi-type lattice with positive and negative Poisson's ratio configurations. *Int J Solids Struct* 2012;49:2450-1209 9.
- 1210 [172] L.Mu. Thiessen polygon. *International Encyclopedia of Human Geography* 2009:231-6.
- 1211 [173] Yamada I. Thiessen polygons. *International Encyclopedia of Geography: People, the Earth, Environment and Technology* 2016. p. 1-6.
- 1213 [174] Cosserat E, Cosserat F. *Théorie des corps déformables* 1909.
- 1214 [175] Lakes RS. Experimental microelasticity of two porous solids. *Int J Solids Struct* 1986;22:55-63.
- 1215 [176] Burns S. Negative Poisson's ratio materials. *Science* 1987;238:551.
- 1216 [177] Ciambella J, Saccomandi G. A continuum hyperelastic model for auxetic materials. *Proc R Soc A-Math Phys Eng Sci* 2014;470:20130691.
- 1218 [178] Gaspar N, Smith C, Evans K. Auxetic behaviour and anisotropic heterogeneity. *Acta Mater* 2009;57:875-80.
- 1220 [179] Koenders MA. Constitutive properties of contacting materials with a finite-sized microstructure. *Mol Simul* 2005;31:873-82.
- 1222 [180] Ciambella J, Bezazi A, Saccomandi G, Scarpa F. Nonlinear elasticity of auxetic open cell foams modeled as continuum solids. *J Appl Phys* 2015;117:184902.
- 1224 [181] Rueger Z, Lakes RS. Cosserat elasticity of negative Poisson's ratio foam: experiment. *Smart Mater Struct* 2016;25:054004.
- 1226 [182] Amores VJ, San Millán FJ, Ben-Yelun I, Montáns FJ. A finite strain non-parametric hyperelastic extension of the classical phenomenological theory for orthotropic compressible composites. *Compos B Eng* 2021;212.
- 1229 [183] Crespo J, Duncan O, Alderson A, Montáns FJ. Auxetic orthotropic materials: Numerical determination of a phenomenological spline-based stored density energy and its implementation for finite element analysis. *Comput Methods Appl Mech Eng* 2020;371.
- 1232 [184] Ren X, Shen J, Tran P, Ngo TD, Xie YM. Auxetic nail: Design and experimental study. *Compos Struct* 2018;184:288-98.
- 1234 [185] Ahmad, Zaini, Mohsenizadeh, Saeid, Alias, Amran, Alipour, Roozbeh. Influence of auxetic foam in quasi-static axial crushing. *Int J Mater Res* 2016;107:916-24.
- 1236 [186] Fei Y, Chen F, Fang W, Xu L, Ruan S, Liu X, et al. High-strength, flexible and cycling-stable piezoresistive polymeric foams derived from thermoplastic polyurethane and multi-wall carbon nanotubes. *Compos B Eng* 2020;199.
- 1239 [187] Zhao J, Wang G, Chen Z, Huang Y, Wang C, Zhang A, et al. Microcellular injection molded outstanding oleophilic and sound-insulating PP/PTFE nanocomposite foam. *Compos B Eng* 2021;215.
- 1241 [188] Zhu S, Zhou Q, Wang M, Dale J, Qiang Z, Fan Y, et al. Modulating electromagnetic interference shielding performance of ultra-lightweight composite foams through shape memory function. *Compos B Eng* 2021;204.
- 1244 [189] Meng D, Liu X, Wang S, Sun J, Li H, Wang Z, et al. Self-healing polyelectrolyte complex coating for flame retardant flexible polyurethane foam with enhanced mechanical property. *Compos B Eng* 2021;219.
- 1247 [190] Li T-T, Dai W, Huang S-Y, Wang H, Lin Q, Lin J-H, et al. Spring-like sandwich foam composites reinforced by 3D Concave–Convex structured fabric: Manufacturing and low-velocity cushion response. *Compos B Eng* 2020;197.
- 1250 [191] Guo K-Y, Wu Q, Mao M, Chen H, Zhang G-D, Zhao L, et al. Water-based hybrid coatings toward mechanically flexible, super-hydrophobic and flame-retardant polyurethane foam nanocomposites with high-efficiency and reliable fire alarm response. *Compos B Eng* 2020;193.
- 1253 [192] Wang L, Wu Y, Li Z, Jiang N, Niu K. Wavy graphene foam reinforced elastomeric composites for

-
- 1254 large-strain stretchable conductors. *Compos B Eng* 2021;224.
- 1255 [193] Carosio F, Negrell-Guirao C, Alongi J, David G, Camino G. All-polymer Layer by Layer coating as
1256 efficient solution to polyurethane foam flame retardancy. *Eur Polym J* 2015;70:94-103.
- 1257 [194] Pan H, Lu Y, Song L, Zhang X, Hu Y. Construction of layer-by-layer coating based on graphene
1258 oxide/ β -FeOOH nanorods and its synergistic effect on improving flame retardancy of flexible
1259 polyurethane foam. *Compos Sci Techno* 2016;129:116-22.
- 1260 [195] Airoidi A, Novak N, Sgobba F, Gilardelli A, Borovinšek M. Foam-filled energy absorbers with auxetic
1261 behaviour for localized impacts. *J Mater Sci Eng A* 2020;788:139500.
- 1262 [196] Yu R, Luo W, Yuan H, Liu J, He W, Yu Z. Experimental and numerical research on foam filled re-
1263 entrant cellular structure with negative Poisson's ratio. *Thin-Walled Struct* 2020;153:106679.
- 1264 [197] Novak N, Krstulović-Opara L, Ren Z, Vesenjak M. Mechanical properties of hybrid metamaterial with
1265 auxetic chiral cellular structure and silicon filler. *Compos Struct* 2020;234:111718.